Oscillatory flow reactors (OFRs) for continuous manufacturing and crystallization

Thomas McGlone,[†] Naomi E. B. Briggs,[†] Catriona A. Clark,[†] Cameron J. Brown,[†] Jan Sefcik[‡] and Alastair J. Florence[,†]*

[†]EPSRC Centre for Innovative Manufacturing in Continuous Manufacturing and Crystallization c/o Strathclyde Institute of Pharmacy and Biomedical Sciences, University of Strathclyde, Technology and Innovation Centre, 99 George Street, Glasgow, G1 1RD, United Kingdom

[‡]EPSRC Centre for Innovative Manufacturing in Continuous Manufacturing and Crystallization c/o Department of Chemical and Process Engineering, University of Strathclyde, 75 Montrose Street, Glasgow, G1 1XJ, United Kingdom

Abstract

Continuous crystallization is an attractive approach for the delivery of consistent particles with specified critical quality attributes (CQAs) attracting increased interest for the manufacture of high value materials including fine chemicals and pharmaceuticals. Oscillatory flow reactors (OFRs) offer a suitable platform to deliver consistent operating conditions under plug-flow operation whilst maintaining a controlled steady state. This review provides a brief overview of OFR technology before outlining the operating principles and summarizing applications, emphasizing the use for controlled continuous crystallization. Whilst significant progress has

been made to date, areas for further development are highlighted that will enhance the range of applications and ease of implementation of OFR technology. These depend on specific application but include scale down, materials of construction suitable for chemical compatibility and encrustation mitigation and the enhancement of robust operation via automation, process analytical technology (PAT) and real-time feedback control.

Keywords

Oscillatory flow reactors, continuous crystallization, manufacturing

TOC

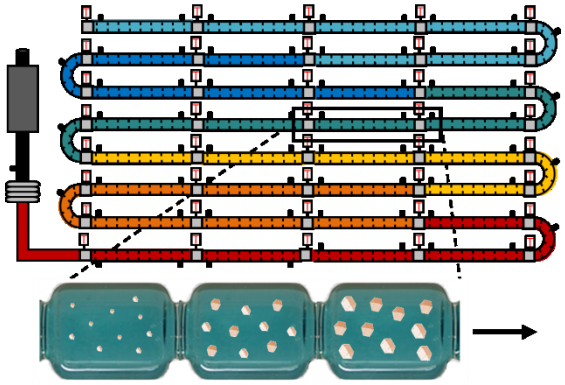

Introduction

Key areas of the chemical industry, including pharmaceuticals, agrochemicals, and dyes/pigments, are still heavily dependent on batch-type processing at the plant scale and little has changed over the last century. The stirred tank reactor (STR) remains the standard approach for mixing, carrying out reactions and crystallizations from early stage discovery to manufacture. Whilst advances in stirring and heat exchange approaches have been implemented in STRs, the adoption of continuous processing for the manufacture of high value chemicals offers a number of potentially attractive benefits that include:

- efficient use of raw materials/solvents[1]

- minimization of waste/disposal[1]
- improved yield/conversion[2,3]
- improved rate/process reliability in addition to enhancing chemical reactions which may have otherwise been limited in a batch-type setup[4,5]
- improved heat/mass transfer with particular suitability towards varying bulk physical forms which exist for specific processes[6,7]
- reductions in energy consumption for running processes in addition to reactor downtime for maintenance and cleaning[8,9]
- efficient use of physical plant space[1]
- significant reduction in process development required for scale up operations[10,11]
- improved handling of hazardous materials including dangerous and/or unstable intermediates[12,13]

The pharmaceutical industry in particular can benefit enormously from the benefits of continuous manufacturing (CM)[14,15] and the availability of microfluidic[16] and mini/mesofluidic reactors which may be used on laboratory and pilot plant scales for development of synthetic processes in particular, provide opportunities to develop and implement continuous processing.[17,18] Reaction parameters such as temperature, concentration and composition of reactants established for a small scale flow process can be directly scaled-up or scaled-out. In contrast, analogous batch-type processes often require significant scale-up design and optimization involving numerous parameters including heat and mass transfer, impeller type and vessel geometry.

In recent years the potential for fully integrated end-to-end CM of pharmaceuticals has been demonstrated for alikserin hemifumarate[19] with all stages from synthesis to final product manufacture carried out in a multi-stage plant that implemented a plant-wide control

approach.[20,21] However there is still a need for further feasibility studies that include assessments of the economical benefits of CM in comparison with batch. It is also worth noting that CM is not the best choice for every process; this is dictated by the inherent kinetic parameters and physical properties of the process. It is also important to note the potential impact of CM on the existing supply chain.[22,23] Whilst there has been a significant rise in flow chemistry research in recent years,[24] for CM to be adopted there is also a need for reactors that can support other operations in continuous mode including work-up, crystallization, filtration, isolation and drying. This review article presents an overview of one technology that is suitable for continuous crystallization processes and covers the general operating principles, considerations for implementation of crystallization, and further requirements.

Crystallization

Crystallization is a complex, multi-phase unit operation used in a wide range of manufacturing industries to achieve separation and purification of products.[25,26] There are various approaches including reactive, evaporative, anti-solvent and cooling crystallization which can be applied depending on the needs of the process. Whichever approach is implemented, delivering control over product purity is critical. Other important targets are yield and particle attributes including size, shape and physical form of crystals. For example, the crystal size distribution (CSD) is commonly used as a critical quality attribute (CQA) and relatively large (e.g. 100 – 500 μm), high quality crystals, which can be reproduced consistently, are typically desired for industrial crystallization processes. Several factors contribute to the final CSD including primary[27] and secondary[28] nucleation, growth, agglomeration, attrition and crystal breakage, encrustation, disturbances to the metastable zone width (MSZW,[26,27,29] see **Figure 1**) such as an impurity profile, polymorphism, agglomeration/aggregation, solvates and hydrates and seeding.

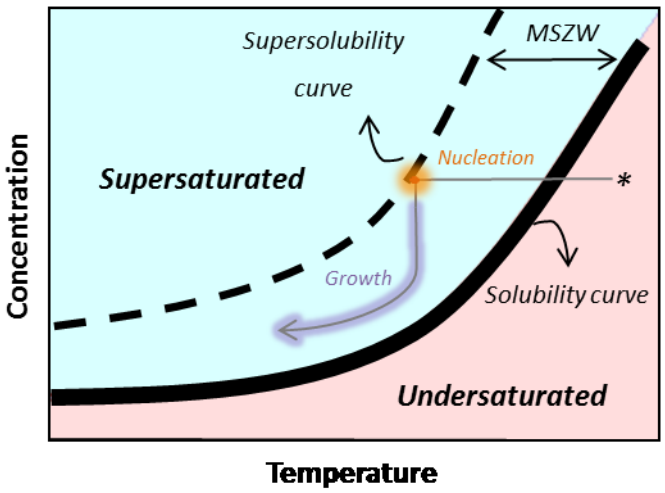

Figure 1. Phase diagram highlighting the supersaturated, saturated and stable undersaturated regions. The MSZW is also shown. The dark, solid line represents a temperature dependent solubility curve.

Conventional approaches for obtaining crystals of a desired crystal form and size distribution have suffered from batch-to-batch variability, particularly at the manufacturing scale. There has been an increasing interest for the pharmaceutical industry in quality-by-design (QbD) approaches[28,30] in order to tackle such variability. Process cost reductions and maximizing operation efficiency are key drivers for exploring these methodologies. Continuous crystallization is an attractive approach for operating via QbD approaches. In addition to the general continuous processing advantages, it offers enhanced control of the physical properties of the crystalline mass.[31] Following a start-up period,[32,33] when a continuous crystallizer is operated under a controlled steady state, the crystallization process in theory behaves under uniform conditions with no variability in temperature, concentration, CSD etc over time leading to greater reproducibility when compared with batch methods. Narrower CSDs obtained directly from crystallization can eliminate the need for further corrective processing such as milling

(highly energy intensive) and have a significant impact on secondary, downstream processes including filtration, drying and subsequent formulation. Furthermore, the control of polymorphic form is an important challenge and the delivery of continuous, consistent process conditions is much more favorable for this purpose.[34] As such there is considerable interest in technologies and approaches that can deliver robust, well controlled continuous crystallization processes.

A number of continuous crystallizer designs are currently in use in the chemical industry, see **Table 1**, although it is noteworthy that these have been significantly less applied for pharmaceuticals/fine chemicals. This may be because many of the advantages of continuous processing are only brought to light when the volumes produced are very large (i.e. commodity chemicals) and most pharmaceuticals compound volumes are relatively low in comparison hence the economic/cycle time drivers are not perceived to be there. In terms of platforms, mixed suspension mixed product removal (MSMPR) setups with single and multiple stages and plug-flow reactors (PFRs) are the most commonly featured. The kinetics of the process should determine platform selection: faster processes with short residence times are favored for PFRs and MSMPR cascades are generally adopted for slower processes requiring longer residence times. In general the principals of PFRs vs MSMPRs have been described elsewhere.[35-39] A typical objective of a series or cascade operation is to economize on heat utilization, e.g. by dividing the overall temperature gradient over several stages and operating each stage at a lower temperature to drive supersaturation. Furthermore, in a cooling crystallization, due to the less extreme temperature drops required across the heat exchange elements, encrustation problems may be significantly reduced. This is a key point as encrustation (defined as the unwanted deposition of solids on a surface) is generally considered the principal reason for disrupting the controlled steady state operation of a continuous crystallizer.

Table 1. Selected literature highlighting various compounds which have been applied for continuous crystallization.

MSMPR (single stage)	MSMPR cascade	Plug-flow
melamine phosphate [40]	Aliskiren hemifumarate[41]	α-lipoic acid-nicotinamide[42]
paracetamol[43]	cyclosporine[44]	industrial API[35]
magnesium ammonium phosphate[45]	pharmaceutical intermediate[46]	ketoconazole, flufenamic acid, *L*-glutamic acid[47]
sodium bicarbonate[48]		calcium carbonate[49]
Deferasirox[50]		benzoic acid[51]
benzoic acid[51]		acetylsalicylic acid[52]
adipic acid[53]		salicylic acid[54]
cyclosporine[55]		
ascorbic acid[56]		
lactose[57]		
sugar[58]		
calcium carbonate[59]		
L-glutamic acid[60,61]		
potassium sulfate[62]		

MSMPRs remain the most utilized platform for continuous crystallization largely due to familiarity in terms of operation and control. These have also been successfully operated at various scales however they pose numerous disadvantages for the application of crystallization including high localized shear regions due to agitators, non-uniform temperature control, challenges with handling solids at transfer lines and non-linear scalability. PFRs offer advantages

in each of these challenges and as a result are interesting platforms for applying continuous crystallization.

History of oscillatory flow reactors

An oscillatory flow reactor (OFR) is a particular type of tubular reactor which has drawn increasing attention over the past few decades.[63-66] It comprises a tubular device containing periodically spaced restrictions (these are commonly orifice baffles although additional types have been investigated)[67,68] superimposed with oscillatory motion of a fluid. Mixing is provided by the generation and cessation of eddies when flow interacts with the restrictions and with repeating cycles of vortices, strong radial motions are created, giving uniform mixing in each inter-restriction zone and cumulatively along the length of the tube,[69] see **Figure 2**. The generation and cessation of eddies has proved to result into significant enhancement in processes such as heat[70,71] and mass[72-74] transfer, particle mixing and separation,[75] liquid-liquid reaction,[76] polymerization,[77,78] flocculation[79] and crystallization, which will be discussed further within this review. Research has been further extended to include flow patterns,[80-82] local velocity profiles and shear rate distribution,[83] residence time distribution (RTD),[81,82,84,85] dispersion,[86-88] velocity profiles[89] and scale-up operations.[90]

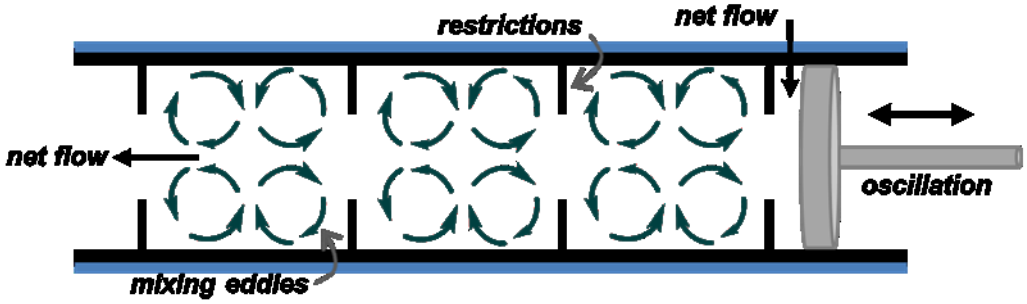

Figure 2. OFR section highlighting fluid mixing on interaction with the equally spaced restrictions. The circular arrows represent idealized fluid flow conditions. In this schematic, oscillation is shown to be provided by a piston.

Whilst this review is fundamentally focused on OFR technology as a platform for continuous crystallization, it was necessary to gather existing literature for additional applications, in order to clearly establish the design rules for construction, operation and scaling. Additionally, the determination of which factors for a given process (be it physical parameters such as density, viscosity, solid loading or kinetic information such as nucleation and growth rates) indicate suitability for implementation into a given OFR system. Traditional crystallization platforms such as MSMPRs or more bespoke platforms such as segmented tubular flow reactors (STFRs)[52,91] or agitated tube reactors (ATRs)[92] may indeed be more appropriate. For example, an OFR may not be able to provide sufficient residence time, the solids loading may be impractical or there may be specific issues with materials of construction. Microreactors (tube diameters of 10 - 500 µm) have received a huge level of interest recently for chemical reactions in flow but are generally less considered for crystallization due to solid handling challenges. This review of OFR technology is particularly timely considering the increasing level of interest in the area, see **Figure 3**.

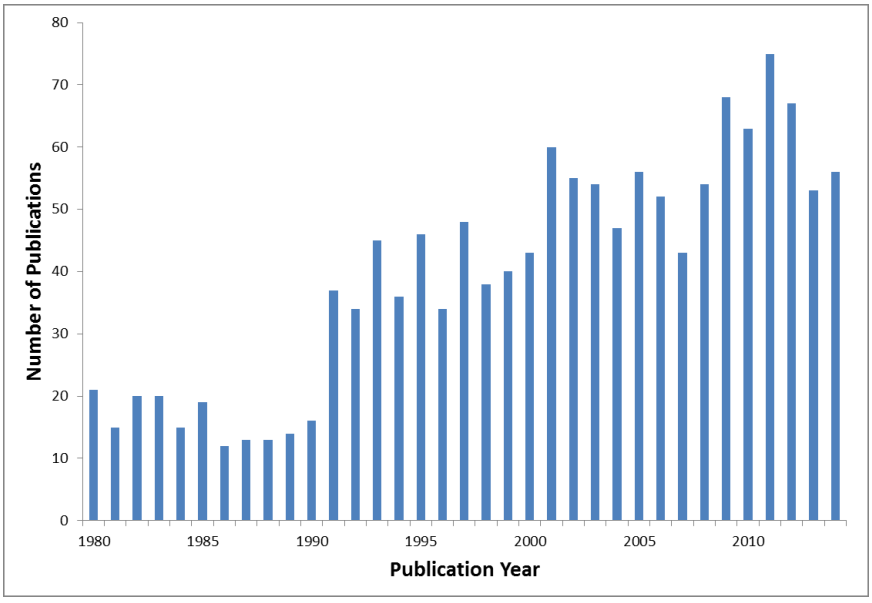

Figure 3. Graph highlighting the increasing level of interest in oscillatory flow reactors. This was generated from Web of Science™ using keywords 'oscillatory flow' and covers a time period from 1980 - 2014.

The general principles associated with OFRs were initially established by Van Dijck in 1935[93] and until the early 1980s, reciprocating plate columns (RPCs)[94,95] and pulsed packed columns (PPCs)[96-99] were the only significant unit operations exploiting the benefits of oscillatory flow mixing, specifically enhanced heat and mass transfer capabilities. Since the 1980s, a number of research groups, and additionally, an increasing number of industrialists, have shown an interest in oscillatory flow reactors due to the highly organized fluid mixing conditions when oscillation is applied.

There are essentially two modes of operation for oscillatory mixing: periodic motion of the intrinsic elements (i.e. moving baffle (MB) or plates) within the column[100-103] or periodic motion of the fluid where the internal elements are fixed.[102,104] These fixed internal constrictions may be inserts which remain stationary or can be engineered within the tubing, a common example being a fully constructed glass system. Examples are displayed in **Figure 4**. For moving fluid (MF) setups an oscillating piston may be used where a plug is coupled to the base of the column.[105] The constrictions are typically spaced at a uniform distance apart and generally, the constriction diameter, d_0, equates to around half the value of the tube diameter.

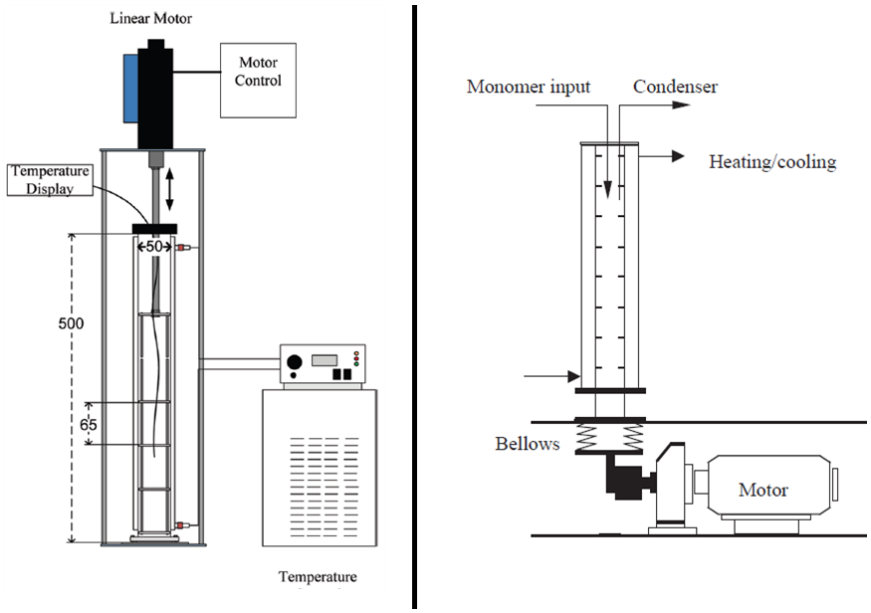

Figure 4. Examples of oscillating platforms. Left: moving baffle (MB)[101] and right: moving fluid (MF).[104]

The most useful, niche application of the OFR has been the conversion of inherently slow reactions from batch to continuous mode with greatly reduced length to diameter ratios (compared to conventional PFRs). Additional advantages have been described including good handling of solids and slurries, enhanced heat and mass transfer capabilities, linear scalability, minimal concentration gradients and facile implementation of process analytical technology (PAT).[106] Limitations have been identified as low tolerance for gaseous species, fluid viscosity and particle density limits, and a threshold for solid concentration. These points will be discussed throughout this review. It should be noted that alternative terminology can often be found in the literature: pulsed flow reactors (PuFRs), oscillatory baffled columns (OBCls), oscillatory baffled crystallizers (OBCs) or oscillatory baffled reactors (OBRs). Ni[65] and Abbot[63] have previously presented reviews on the applications of oscillatory flow technology, the contribution by Ni in 2003 summarizing the concepts and key developments of OFR enhancement and by Abbot in

2013, with a specific focus on biological processing. McDonough has also reviewed mesoscale OFRs for rapid process development.[107] There have also been numerous PhD theses dedicated to the subject.[87,108,109]

OFR operating principles

Whilst conventional tubular reactors rely on a high throughput velocity to achieve mixing i.e. obtaining the net velocity to achieve a high enough *Reynolds number* (*Re*, defined below for an STR and pipe in **Equations 1** and **2**) potentially resulting in excessive tube lengths to accommodate long residence times, an OFR system does not. In this case, the flow conditions are governed by the effect of the oscillations. The periodically reversing fluid motion which interacts with the baffles forms strong toroidal vortices, hence allowing lower net flow velocity and shorter tubing lengths in addition to lower working volumes when compared to conventional systems. In **Equations 1** and **2**, Re_{STR} is the Reynolds number for a stirred tank reactor, Re_{pipe} is the Reynolds number for flow through a tube, N is the impeller speed, D_{imp} is the agitator diameter, ρ is the fluid density, μ is the dynamic viscosity, u is the net flow velocity and d is the tube diameter.

$$Re_{STR} = \frac{\rho N D_{imp}^2}{\mu} \quad (\mathbf{1}) \qquad Re_{pipe} = \frac{\rho u d}{\mu} \quad (\mathbf{2})$$

Operating under plug-flow conditions means that the residence time in a given reactor is the same for all elements of the fluid, see **Figure 5**. Plug-flow is defined as an orderly flow of fluid through a reactor and the key aspects are (i) no overtaking fluid elements in the direction of flow, (ii) perfect mixing in the radial direction and (iii) that all flow elements reside for the same length of time. This has been related to crystallization via various modelling approaches.[47,110-112] Traditionally, near plug-flow conditions have been achieved using a series of MSMPRs with the theory that plug-flow is achieved when the number of reactors approaches infinite. The

disadvantages of this include higher overall running costs, a lack of temperature control for transfer lines (although this can be addressed to some extent) and, specifically for crystallization reactions, particles may be broken up or retained within pumps causing undesirable nucleation events and blockages. Near plug-flow conditions have also been obtained by operating a tubular reactor at turbulent flow, the major disadvantage being the need for significantly high flow rates (short residence times) leading to very long reactors and large capital costs.

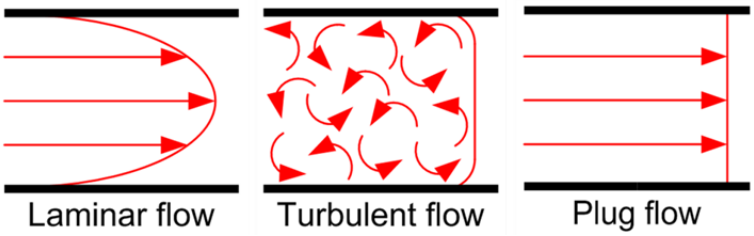

Figure 5. Illustration of laminar, turbulent and plug-flow.

The unique mixing effect generated by oscillation is generally achieved across typical ranges of 0.5 - 20 Hz (frequency, f) and 1 - 100 mm (center-to-peak amplitude, x_0). The MB approach tends to be limited to batch-type setups whereas MF is adopted for both batch and continuous. Changing the combination of f and x_0 allows control of the generation of eddies and produces a range of fluid mechanical conditions as broad as required.[69,113,114] For continuous operation, the oscillation can be generated at one or both ends of the column using bellows, pistons or diaphragms.

When considering continuous operation, the system should be operated such that the maximum oscillatory velocity is at least double the net velocity of the fluid flowing through the tube. This means that the flow is always fully reversing with the fluid interaction at the constrictions. The mixing generated in the zones between successive constrictions is then uniform, and the tube itself can behave as a series of well mixed stirred tanks. Importantly, mixing is independent of

the throughput velocity meaning it is possible to have a low net flow velocity (corresponding to nominal laminar regime in the absence of oscillations), but maintain good mixing and plug-flow performance through control of the oscillatory conditions.

Various approaches for imposing periodic constrictions in an OFR have been reported in the literature including single and multi-orifice baffles and smooth periodic constrictions (SPCs). Single orifice baffles are the most commonly encountered at various scales whereas the SPC systems are a more recent development and are mainly limited to mesoscale platforms with the exception of one study.[115] These will be discussed in detail later on. Multi-orifice systems have been shown to exhibit a higher degree of similarity in terms of shear rates and mixing intensity when scaling up in comparison to single orifice platforms.[67,68,116] The presence of SPCs as opposed to 'sharp-edge' baffles has been shown to minimize high shear regions and maximize mixing efficiency with the elimination of 'dead-zones' in which particles may sediment or become trapped.[117]

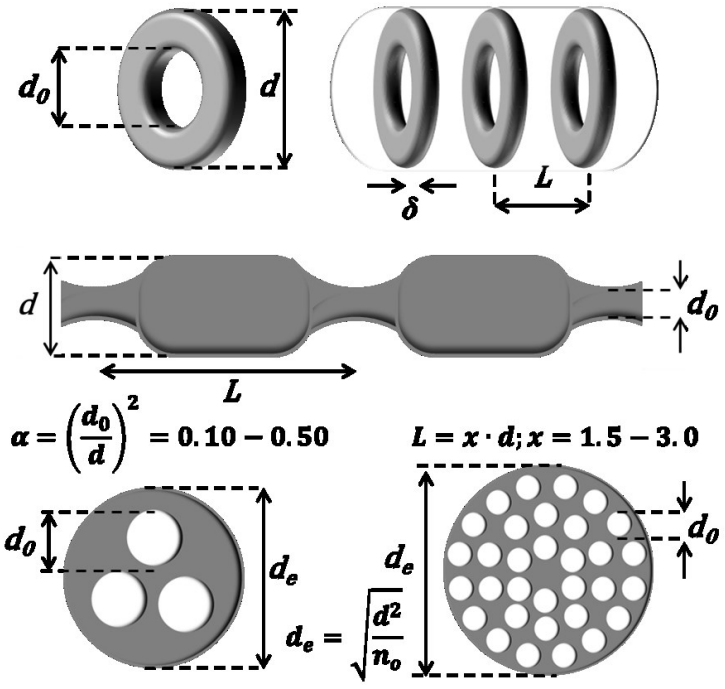

Figure 6. Schematic illustrating the various approaches in the literature for imposing constrictions in an OFR. Top: single orifice baffle designs, middle: smooth periodic constrictions (SPCs) and bottom: multi-orifice baffle designs. The equations for calculating the baffle open cross sectional area, α, baffle spacing, L, and effective tube diameter, d_e are also shown.

The constriction spacing, L, is normally within the range of 1 - 3 times the tube diameter, with a distance of 1.5 d being the most common due to interpretation of flow visualization photographs by Brunold[80] for effective mixing over a wide range of f and x_0. Ni later identified L = 1.8 d as an optimal spacing based on a mass transfer study.[90] Different values of L will result in different flow behaviors as the shape and length of the eddies are influenced within each constriction cavity.[118] Mackley used a new dimensionless group called the stroke ratio intending to classify the flow in terms of the relation between oscillation amplitude and L.[119] The optimal L should ensure a full expansion of vortex rings generated behind constrictions so that vortices will spread effectively throughout the entire inter-constriction zone. At a small value of L the generation of vortices is strongly suppressed. This effectively restrains the growth of vortices and reduces the required radial motion within each constriction cell. If the constrictions are spaced too far apart, the vortices formed behind the constrictions cannot effectively cover the entire inter constriction regions. Stagnant plugs in which vortices will disperse and diminish.

The baffle open cross sectional area, α, is normally chosen within a range of 10 - 50 % based on a compromise between minimizing frictional losses and maximizing the mixing effect. Various studies[77,114] have been carried out in attempt to optimize this parameter including a systematic investigation by Gough[69] for polymerization suspension mixing. At lower values ~26 % small symmetrical eddies were formed at the sharp edges of the baffles and the vortex rings did not encompass the entire column cross section nor the complete length of the entire baffle

region, thus stagnant regions between eddies were identified. Increasing to ~32 %, eddies extended to the reactor walls covering a greater area of the section. Vortex rings were still symmetrical along the center line (axi-symmetric) and displaying small interaction. Increasing to 40 % the axi-symmetry was lost and the intense interaction between eddies led to the disappearance of the stagnant regions within the baffled cavity – inducing plug-flow characteristics desirable for continuous operation. At the highest values ~47 %, a large degree of channeling through the baffle orifice was observed and the formation of eddies was destroyed by the predominant axial movement, thus low mixing took place.

In terms of scaling between OFR systems, L and α (**Figure 6**) are crucial parameters which must be kept constant in order to minimize any process development scale up issues, as these factors control the size and shape of the resultant mixing vortices.[120] They are calculated via **Equations 3** and **4.** Note that an effective tube diameter term, d_e, is used for multi-orifice systems.[109]

$$L = 1.5\,d \quad (\mathbf{3}) \qquad \alpha = \left(\frac{d_0}{d_e}\right)^2 \quad (\mathbf{4}) \qquad d_e = \sqrt{\frac{d^2}{n_o}} \quad (\mathbf{5})$$

In general, the overall fluid mechanical conditions of an OFR are governed by two dimensionless quantities,[121] namely the oscillatory Reynolds number, Re_0 and the Strouhal number, St, as shown in **Equations 6** and **7** below:

$$Re_0 = \frac{2\pi f x_0 \rho d_e}{\mu} \quad (\mathbf{6}) \quad St = \frac{d_e}{4\pi x_0} \quad (\mathbf{7})$$

Re_0 describes the intensity of mixing applied to the tube, where $2\pi f x_0$ equates to the maximum oscillatory velocity (ms^{-1}), and St is the ratio of column diameter to stroke length (or amplitude), measuring effective eddy propagation inside the baffle cavities.[80,121-124] St is inversely proportional to x_0 and if too high, causes eddies to be propagated into the adjacent cavities. In

contrast to steady flows in pipes, where the transition to turbulence begins at around Re = 2000, flow separation in oscillatory flows occurs for values of Re_0 of the order 50.[125] At low Re_0 = 100 – 300 the system exhibits plug-flow characteristics where vortices are axi-symmetrically generated within each baffled cavity. This is generally known as a soft mixing regime. When Re_0 is increased further symmetry is broken and flow becomes intensely mixed and chaotic, i.e. more turbulent like.[78,126] The net flow Reynolds number, Re_n, analogous to Re_{pipe} but with u representing a superficial net flow velocity, can be calculated via **Equation 8** as follows:

$$Re_n = \frac{\rho u d}{\mu} \quad (\mathbf{8})$$

Re_n is fixed by u and Re_0 is fixed by the intensity of oscillation. There is little advantage in using oscillatory flow if Re_n > 250 as the effects of net flow become significant and the benefits of operating at laminar flow rates diminish.[125] The calculation of Re_n allows a velocity ratio, ψ to be determined via **Equation 9**:

$$\psi = \frac{Re_0}{Re_n} \quad (\mathbf{9})$$

This ratio should be greater than 1 so that the maximum oscillation velocity is always higher than the net flow velocity through the tube, however values in the range of 2 - 10 have been recommended for plug-flow operation.[66] It should be noted that these values have only been validated for liquids as opposed to multi-phase systems such as slurries. A major property of oscillatory flow mixing is that secondary flow (i.e. flow reversing) occurs only in the vicinity of tube constrictions. As a consequence, the fluid back-mixing[127] generated by the oscillatory movement of the fluid in the plain sections of the tube should be negligible. An approach for continuous operation therefore would be to fix the flow velocity, i.e. the fluid rate being pumped through the tube, hence securing the residence time for a given tube size and length, and

subsequently choosing the oscillatory conditions such that $Re_0 > Re_n$ ($\psi > 1$) meaning that the superimposed oscillations will dominate the mixing regime. It should be noted that minimum values for Re_n and Re_0 of 50 and 100 respectively have been postulated for sufficient mixing.[66]

OFR systems are often compared to STR 'equivalents' considering power density values, P/V ($W\ m^{-3}$), i.e. the amount of power applied per unit volume for each system. Power density values have been typically used when scaling between STR setups and for an STR this is defined via **Equation 10** as:

$$\frac{P}{V} = \frac{P_0 \rho N^3 D_{imp}^5}{V_L} \quad (\mathbf{10})$$

P_0 is the power number, D_{imp} is the impeller diameter and V_L is the volume of liquid in the STR. P_0 can be calculated[128] or derived from plots generated by agitator suppliers and is dependent on Re_{STR}. There are normally corrections applied for variations such as agitator, baffling and reactor type.

There are essentially two models for estimating the power density in an OFR: the quasi-steady flow model[129] and the eddy acoustic model.[130] The power input for the eddy acoustic model is justified for conditions of low x_0 and high f e.g. 1 - 5 mm, 3 - 14 Hz. This can be calculated using **Equation 11** where l_e is defined as the mixing length for the eddy enhancement model.

$$\frac{P}{V} = \frac{1.5(2\pi f)^3 x_0^2 l_e}{L\alpha} \quad (\mathbf{11})$$

The quasi-steady flow model was originally derived for packed columns and subsequently used for pulsed columns.[131] The power input for this model is valid for higher x_0 and lower f values e.g. 5 - 30 mm, 0.5 - 2 Hz and can be estimated from **Equation 12** below.

$$\frac{P}{V} = \frac{2\rho N_b}{3\pi C_D^2}\left(\frac{1-\alpha^2}{\alpha^2}\right) x_0^3 (2\pi f)^3 \quad (\mathbf{12})$$

N_b is the number of baffles per unit length of tube and C_D is the coefficient of discharge of the baffles (directly related to the orifice in the baffle and has a normal value of 0.7).

An OFR offers enhanced heat transfer capabilities when compared to conventional tubular systems as the presence of oscillation and baffles impacts a significant change in the fluid mechanical conditions. When considering, for example a cooling crystallization process, one could envisage significant benefits in terms of heat exchange whilst at the same time maximizing energy efficiency. For a shell and tube heat exchanger (i.e. jacketed tube), where a fixed mass of fluid in the tube is cooled or heated by the flow of a fluid of given temperature through the shell, the tube-side Nusselt number, *Nu*, can be calculated via **Equation 13**:

$$Nu = \frac{h_t d}{k} \quad (\mathbf{13})$$

k is the thermal conductivity of the fluid and h_t is the tube-side heat transfer coefficient. Many additional factors have to be considered including the thermal conductivity of the tube wall material, the outer tube diameter, the specific heat capacity of the fluid, flow rates, the total area for heat transfer as a function of the tube diameter and (if applicable) any encrustation implications. Various studies have been completed demonstrating enhancement of *Nu* values via comparisons of unbaffled and baffled systems in addition to the presence and absence of oscillations.[70,71] The effects of Re_0 have also been reported (see **Figure 7**) and the heat transfer rate shown to be strongly dependent on the product of f and x_0. Furthermore, comparisons have been made between MB and MF systems[132] illustrating that for both oscillatory configurations the heat transfer performance at minimum matched that of a turbulent pipe whilst being able to operate in laminar flow regimes.

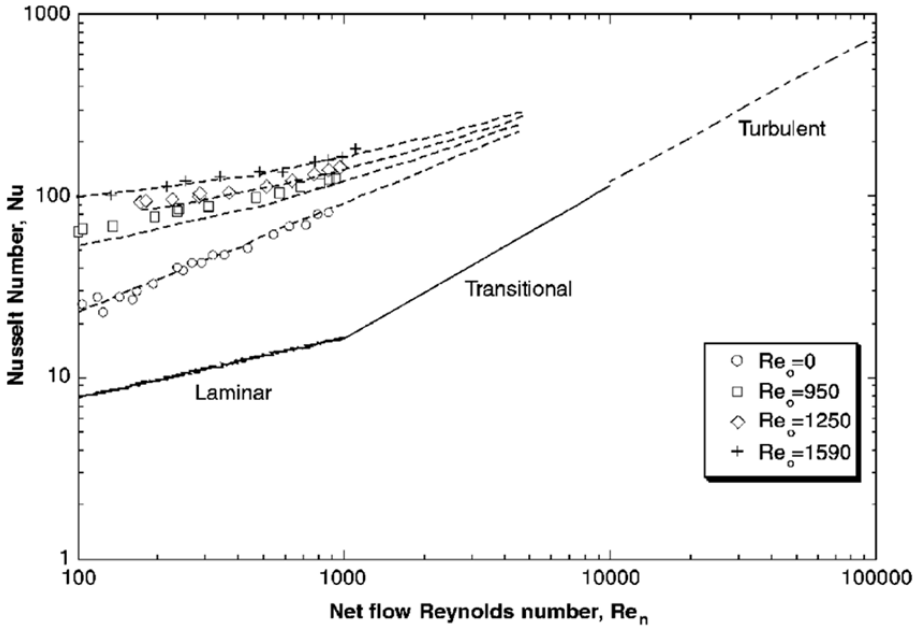

Figure 7. Diagram illustrating heat transfer enhancement in an OFR. Reproduced with permission from reference 65. Copyright 2003 Elsevier.

Improved mass transfer is often described for OFR systems when considering alternative mixing devices such as STRs.[73] This has been studied primarily via gas-liquid investigations[131,133-135] (although alternative approaches have been described)[136] and the mass transfer of gas into liquids is normally quantified using k_La, the volumetric mass transfer coefficient that describes the efficiency of this transfer. Comparisons have been made in the presence and absence of baffles and oscillations, improved gas hold up and contacting has been observed for various baffle designs, and power density correlations have illustrated advantages in mass transfer for OFR systems in comparison to STR setups due to improved shear rate distributions.[73] Mass transfer enhancement has also been shown to be strongly dependent on the specific f and x_0 conditions and interestingly, linear scale up as a function of mass transfer has been demonstrated for batch OFR platforms.[90] Further studies have included investigations at

various fluid viscosities[137] and the demonstration of mass transfer enhancement with multi-orifice platforms compared to single orifice.[116]

With the rapid advancement of computational fluid dynamics (CFD) modelling, studying the flow and transport phenomena in an OFR has become feasible. Furthermore, these CFD models have often been used in conjunction with particle imaging velocimetry (PIV) resulting in a powerful approach towards characterizing the fluid mechanics of the system. Early studies[87,123,138-140] revealed that the vortex mixing mechanism was responsible for the high mixing efficiency of the system and predictions of the onset of chaotic motions and concentration gradients were evaluated by incorporating transport such as heat and mass transfer and provided fluid-particle motion simulations.[81,141,142] As mixing eddies have been shown to be the essential enhancer, large eddy simulations (LESs)[67,143,144] have been particularly suited for studying flow in an OFR and the effects of f and x_0 have been investigated.

The flow characteristics of oscillatory flow are dominated by the axial velocity components (see **Figure 8**) but with numerical studies there is now good understanding of the nature of the mixing.[145-149] At Re_0 = 100 - 300, the OFR exhibits good plug-flow characteristics where the vortices are axi-symmetrically generated within each baffled cavity (referred to as plug-flow mode). For higher Re_0 values the generation of vortices is no longer axi-symmetrical and the flow becomes intensely mixed and chaotic (referred to as the mixing mode). Depending on column geometry and viscosity these critical values may vary.[150]

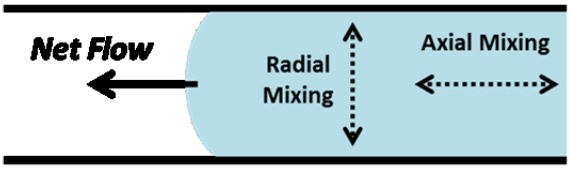

Figure 8. Illustration of axial and radial dispersion for flow within a tubular system.

As the oscillatory motion is periodic and fully reversing, there are two half cycles, each containing flow acceleration and deceleration corresponding to a sinusoidal velocity-time function. On each flow acceleration, vortex rings form downstream of the baffles. A peak velocity is reached, and then as the flow decelerates, the vortices are swept into the bulk, and subsequently unravelled with the bulk flow acceleration in the opposite (axial) direction. It is the strong radial velocities, arising from the repeating cycles of vortex formation and of similar magnitude to the axial velocities, that give uniform mixing[151] in each inter-baffle zone and cumulatively along the length of the column.

Various CFD studies have been reported including comparisons with baffled and unbaffled systems illustrating the challenges in achieving efficient radial mixing at low flow rates.[152-154] Comparisons of MB and MF systems have also been performed,[155] in addition to scaling studies between OFRs.[156] Simulations incorporating oscillatory flow highlighted an efficient way of generating well mixed flows with low axial dispersion, good global mixing with high shear rates at the walls and hence a near plug-flow residence time distribution (RTD) is achievable at Re_n values as low as 80.[154] Furthermore, CFD models in conjunction with PIV have been used to correlate strain rate with the power dissipation generated within OFRs and lower strain rates were calculated for OFRs in comparison to STRs at similar power density values.[83,157] Comparative experiments have shown that volume averaged shear rates for OFRs are an order of magnitude larger than that of an STR and particles in an OFR spend most of their residence time in high shear regions.

In general, the way in which RTD can be affected by manipulation of the mixing conditions is fundamental to the operation of a reactor.[158] For OFRs the RTD performance can be affected independently of the net flow conditions, i.e. very sharp (or near plug-flow) RTD measurements

can be achieved at moderately low Re_n values as a result of radial velocity components being of comparable magnitude to the axial velocities in a tubular system.[159,160] The axial dispersion coefficient, D is used to describe the characteristics of mixing in tubular setups. It is a measure of the degree of deviation in flows from the true plug-flow scenario: in theory D should be zero for plug-flow. **Equation 14** shows a species material balance subject to transport by convection and axial dispersion in a one dimensional continuous system:

$$\frac{\delta c}{\delta t} = D\frac{\delta^2 c}{\delta^2 x} - u\frac{\delta c}{\delta x} \quad (\mathbf{14})$$

c is the concentration of the species, t is the time and x is the position along the axial length Three types of model have been used in the literature[161] to study RTD in an OFR: a dispersion model-type where the reactor is seen as a one dimensional continuous path, a compartmental (tanks-in-series) model-type in which the reactor is considered as being divided into well-mixed discrete stages and a tanks-in-series incorporating back-mixing. The concept of an 'ideal' STR assumes the composition of fluid leaving the tank is equal to the average composition within the tank. The tanks-in-series model considers each inter-baffle zone as an STR and the model assumes the concentration-time response can be represented by a cascade of equal size, 'ideal' STRs in series which gives the best fit to the concentration-time data. When the deviation from plug-flow is small, the dimensionless axial dispersion coefficient term[36] (or inverse Peclet number), D/ul can be related to the number of stirred tanks in series, n, via **Equation 15**:

$$\frac{D}{ul} = \frac{1}{2n} \quad (\mathbf{15})$$

l is the length of the tubular vessel. Ideally, a continuous OFR (COFR) should be operated at an x_0 value that gives the minimum D/ul. Considering a large number of continuous stirred tanks in series, with net flow and an overall plug-flow response, such a system may be of great benefit

to processes such as crystallization where the lifetime of each given particulate can be maintained resulting in a very narrow CSD, see **Figure 9**. The nature of the fluid mechanics ensures good radial mixing within the tube and the level of axial dispersion depends in particular on both Re_0 and St.

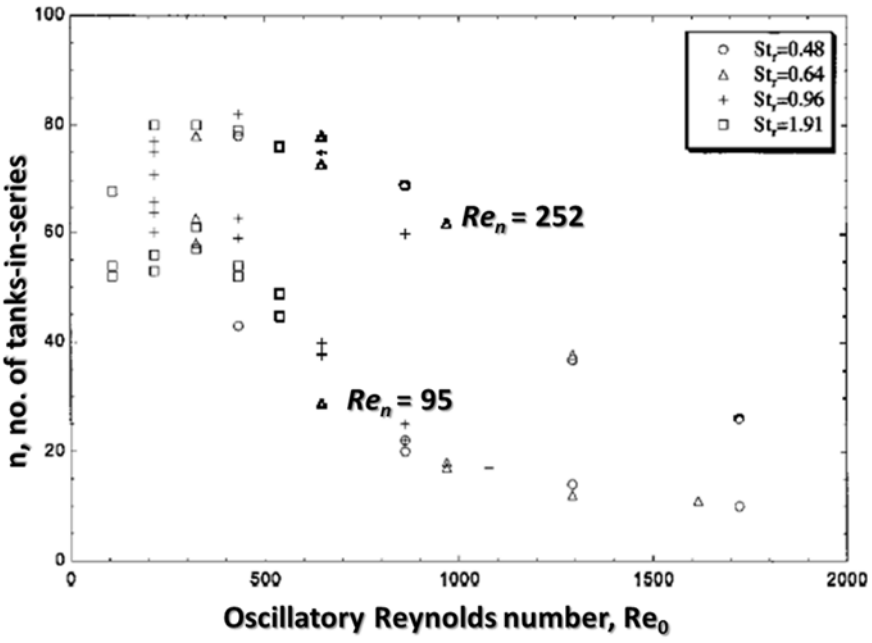

Figure 9. Plot showing the dependency of the number of tanks-in-series, n vs Re_0 on St. Reproduced with permission from reference 125. Copyright 2003 Elsevier.

When oscillations and baffles are present, D is relatively insensitive to Re_0 but is influenced by x_0 as this controls the length of eddy generated along the tube. Dispersion, using oscillatory flow and baffles, can be compared with that obtained by running the tube with a turbulent net flow. When Re_n is high, the presence of baffles makes little difference to the dispersion. However, the absolute value of dispersion in a turbulent net flow can be considerably higher than that using oscillatory flow with baffles at a lower Re_n. This implies that, for a given residence time requirement, a narrower RTD can be achieved using oscillatory flow and baffles over a turbulent net flow.

Experimental RTD studies for various OFR systems have been reported via tracer injections[84,162] (although alternative approaches have been considered)[163] and monitoring some response as a function of time. An imperfect pulse correction can be applied to the modelling approaches in order to incorporate experimental technique.[81,82,85,88] The effect of tracer density has also been investigated.[126] The application of oscillation has a significant impact on the RTD of a given system; an absence of oscillation results in concentration curves typical of those observed for laminar flow in a tube e.g. a sharp breakthrough followed by a decay curve with a long tail corresponding to the arrival of fluid elements that have travelled in different radial positions and consequently have moved through the tube with velocities less than the centreline peak velocity. We have performed numerous RTD characterisations on COFR systems, the details of which are published elsewhere,[164] in order to identify the level of deviation from plug-flow operation, see **Figure 10**. This specific example is for a 15 mm COFR system with an aqueous medium and tracer injection modelled with the Levenspiel perfect pulse model. An optimal RTD response can be observed from various oscillatory and net flow conditions.

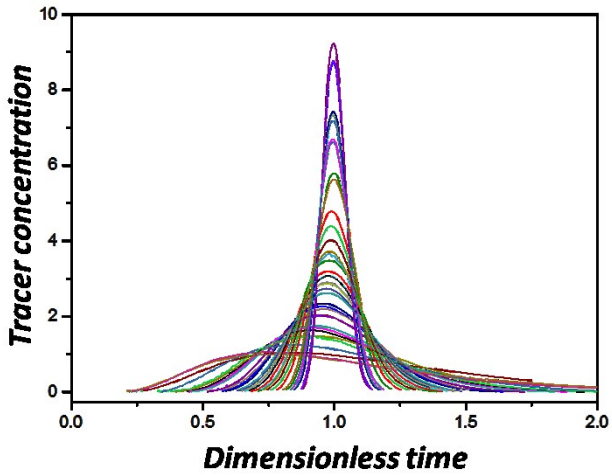

Figure 10. Plot showing tracer concentration as a function of dimensionless time as predicted by the perfect pulse model for various operating conditions of a COFR. An optimal region close to plug-flow can be observed.

The effects of f and x_0 on the RTD have also been investigated[84] and in general x_0 has a more pronounced effect on the dispersion characteristics, see **Figure 11**. It has been shown that a well-defined region for Re_0 exists where the RTD is closest to plug-flow behaviour for any fixed Re_n and it was found that the velocity ratio in the range $2 < \psi < 4$ corresponded to the optimal RTD conditions being achieved.[125] These dimensionless parameters are sufficient to select the oscillatory conditions necessary to obtain an optimum RTD in an OFR based on a desired throughput specification.

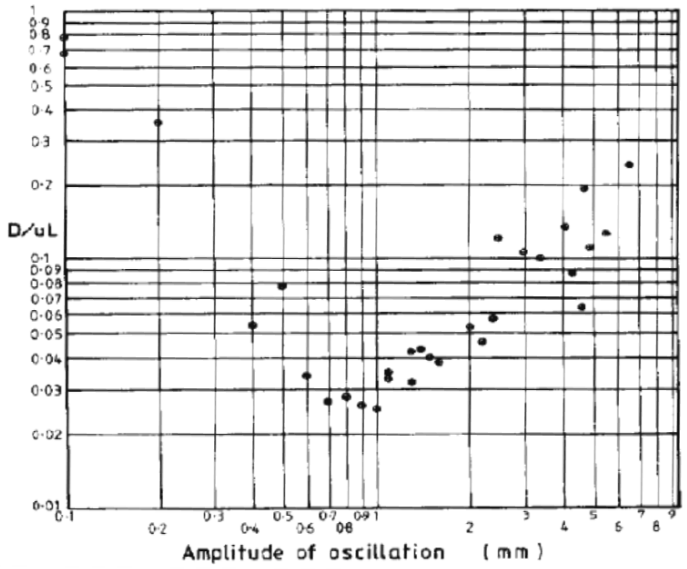

Figure 11. Graph of log dispersion D/ul as a function of log amplitude of oscillation. Reproduced with permission from reference 84. Copyright 2003 Elsevier.

A summary of the desirable operating ranges for traditional OFRs is shown below in **Table 2**.

Table 2. Summary of the accepted ranges for Re_0, St, Re_n and ψ for traditional OFRs based on the existing literature.

Re_0	St	Re_n	ψ
50 (flow separation occurs)[125]	< 0.1 (fast stream core, strong shear)[149]	> 50 (minimal value for convection i.e. sufficient mixing)[66]	> 1 (maximum oscillatory velocity higher than net flow[66] velocity)
> 100 (minimal value for convection i.e. sufficient mixing)[66]	> 0.5 (effective eddy shedding)[149]	> 80 (rapid mixing and uniformity)[142]	2 - 4 (optimal RTD conditions)[66]
< 250 (flow 2-D, axi-symmetric, soft mixing regime)[159]	0.6 – 1.7 minimum axial dispersion coefficient, D[84]		
> 250 (flow 3-D, no axi-symmetry, turbulent-like)[159]			

Equipment

The application of OFR technology has increased in parallel with the development of suitable equipment and robust platforms which are able to exploit the various advantages. **Table 3** highlights a selection of patents (associated with crystallization) which have been filed representing various technical advances.

Table 3. Summary of patents filed relevant to OFRs and crystallization.

Patent	Summary	Filing Date	Inventor(s)	Reference
Incrustation resistive crystallizer	Vibrating perforated plates for encrustation mitigation	Feb, 1984	Carter, Hsu	EP 0119 978 A2
Oscillatory flow mixing reactor	Mixing for multiple phase systems	Feb, 2006	Gron, Schutte, Drauz, Stadtmüller, Grayson	US 2008/0316858 A1
Improved apparatus and method for temperature controlled processes	Controlled temperatures applied to a substance in different process zones	Nov, 2006	Ni, Laird, Liao	WO 2007060412 A1

Apparatus and process for producing crystals	COBC for crystallisation including ultrasound	Jan, 2010	Ruecroft, Burns	US 2011/0288060 A1
Crystallisation process and apparatus	Oscillatory based continuous crystallisation platform with automated control	Oct, 2010	Harji	WO 2011051728 A1
Oscillating flow minireactor	Oscillating flow device with directional changes in a channelled pathway	Jan, 2011	Reintjens, Thathagar	US 2014/0081038 A1
Device for inducing nucleation	Surface abrader configured to induce crystal nucleation within a vessel	Dec, 2012	Ni, Callahan	WO 2013088145 A1

The majority of early studies featured batch-type OFR setups for various applications including bio-[105,165,166] and chemical reactions,[76] polymerization,[78,167,168] photo-catalysis,[169-171] flocculation,[79,172] gas-liquid contacting,[173] phase-transfer catalysis (PTC),[174] hydrate formation[175] and mitigation of wax deposition.[176] For polymerization applications, some interesting correlations have been made between droplet size (as a function of f and x_0) and the polymer particles.[104] There has been significant interest in OFR platforms for biological applications and *process intensification*[177] i.e. the development of novel apparatus and techniques to bring dramatic improvements in manufacturing and processing, substantially decreasing equipment size/production capacity ratio, energy consumption, or waste production. Additionally, while the majority of these applications involved a single orifice baffle design, alternative approaches have also been considered.[178]

The OFR has also been examined for continuous applications, see **Figure 12**. Ni used a 25 m glass system (d = 40 mm) to evaluate droplet size distributions (DSDs) of oil/water mixtures over a range of f and x_0 values.[179-181] Stonestreet evaluated a pilot scale stainless steel OFR of 2.9 m (d = 24 mm) length as a method for continuous production of sterols in an ester saponification reaction.[182] The COFR achieved the required product specification, in a residence time one eighth that of a full scale batch reactor. Harvey used a 3 m (d = 25 mm) glass COFR to

investigate the trans-esterification of natural oils to form biodiesel in a process intensification trial.[183] It was demonstrated that a suitable conversion could be achieved in a residence time substantially lower than that of batch processes. Vilar used a glass 5 m (d = 50 mm) COFR to study oil/water emulsions with electrical impedance tomography (EIT) as an on-line analytical tool.[184] This allowed concentration mapping and the measurement of velocity distributions in two-phase flows, where electrical conductivity or permeability differences exist between the two-phase fluids. Very recently, Lobry utilized a 5 m glass COBR (d = 15 mm) for liquid – liquid dispersion towards suspension polymerization of vinyl acetate.[185]

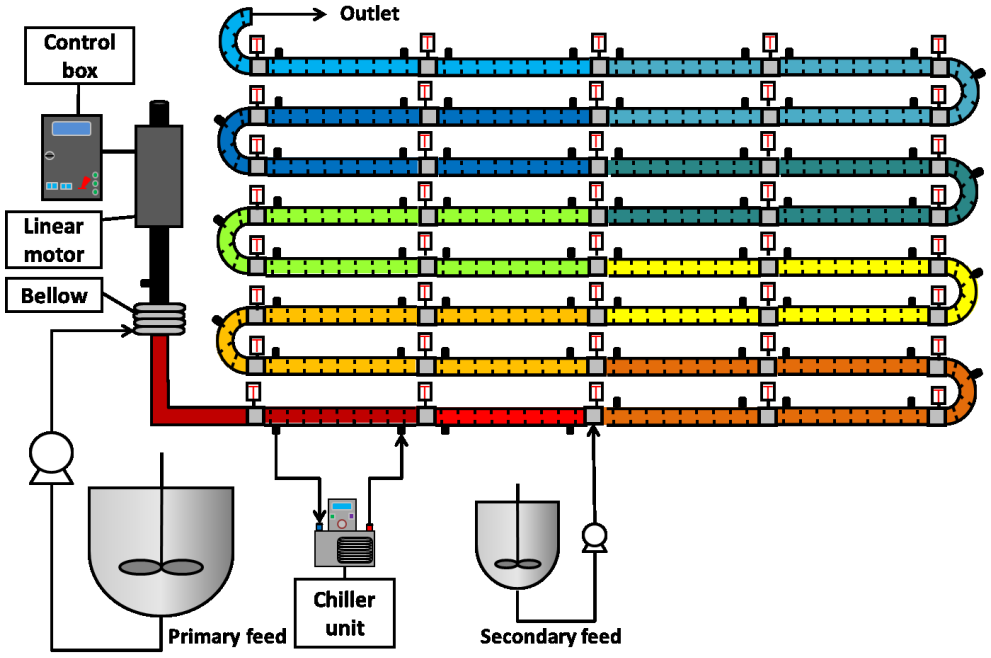

Figure 12. Schematic of a continuous OFR setup.

Within the last decade there has been significant development in *mesoscale* OFRs[117] for the scaling down of processes. These have been designed to be scalable towards industrial application directly or to be used as independent, small scale production platforms. A critical difference between these systems and conventional OFRs, in addition to the smaller working tube diameter, is the presence of SPCs as opposed to 'sharp-edge' baffles. While conventional

OFRs are linearly scalable[113,186] with respect to parameters L and α, the fluid mechanics at $d < 10$ mm are behaving differently and questions around solid loading are critical, particularly when considering high throughput continuous operation. Interestingly, a minimal value of Re_n was found to be around 10 (equating to flow rates of less than 10 ml min^{-1} although lower flow rates have been investigated) for these systems as compared to 50 for conventional OFRs[66] potentially allowing for considerable residence times to be achieved.

The fluid mechanics within a mesoscale OFR do have some similarities to those generated in conventional OFRs, but with a decreased critical Re_0 number of 100 for flow separation and breakage of flow axi-symmetry which was found to be related to the smaller cross-free section of the constrictions in the SPC geometry. Numerical simulations[187] with a 2-D axi-symmetric laminar model have matched the flow patterns within the SPC geometry for situations with small interaction between fluid elements (axi-symmetric flow) while a 3D model (laminar or LES)[187] was necessary to match the breakage of flow axi-symmetry observed for higher values of Re_0. The fluid mechanics in the mesoscale systems were also found to be more sensitive to x_0 and this has been mainly attributed to the differences in baffle geometries.

The effect of oscillatory flow in a mesoscale screening reactor with regards to RTD of the liquid phase has been demonstrated using a reactor formed by several jacketed glass tubes, each of length 35 cm (d = 4.4 mm) and a volume of *ca.* 4.5 ml.[188] The SPCs were positioned with a mean spacing of 13 mm (approximately 3 d) and a constriction length of 6 mm. The constriction diameter was 1.6 mm, representing 13 % (α = 0.13) of the cross-sectional area. This is considerably less than the 50 % cross-sectional area used in conventional OFRs (α = *ca.* 0.2). The results of the study showed that the level of back-mixing was highly dependent on both f and x_0 (as with traditional OFRs) and x_0 had a higher effect than f. This work has been extended

using a combination of PIV and CFD for evaluation and a correlation fitted to experimental data has allowed an empirical approach for estimation of axial dispersion in the mesoscale system,[187] see **Figure 13**. At optimal oscillation conditions (f = 12 Hz, x_0 = 4 mm) the mixing observed at larger scales could be reproduced at this smaller scale and interestingly, it was possible to keep high concentrations (15 wt./wt. %) of small diameter polymer supported catalyst beads suspended in the screening reactor whilst maintaining uniform fluid mixing. Importantly, the oscillation conditions have been shown to exhibit a strong influence on the RTD at Re_n < 10 and little effect on the RTD curves at Re_n > 25.[189,190]

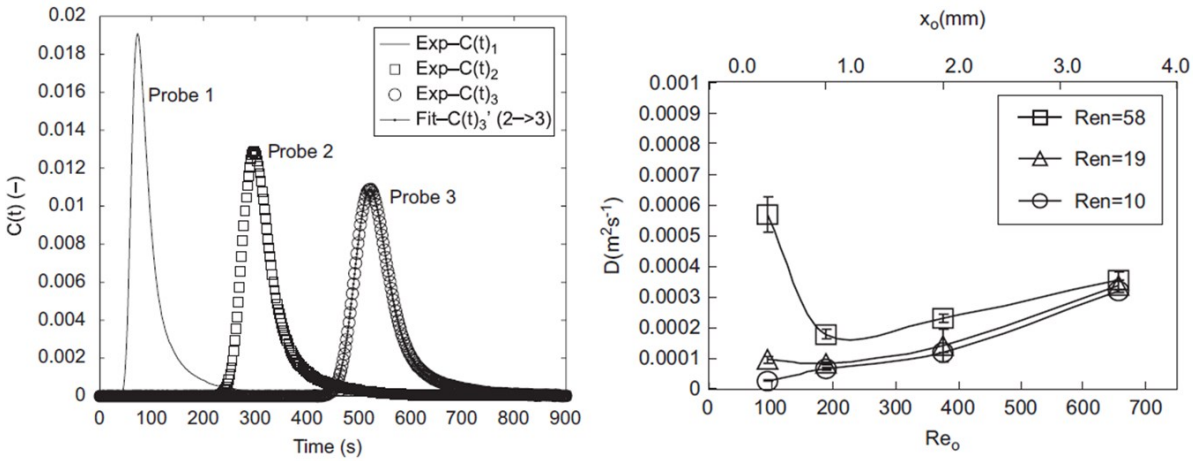

Figure 13. Left: experimental normalized *c*-curve and dispersion model fitting by imperfect injection method. Right: axial dispersion coefficient (D) as a function of Re_0 for a fixed oscillation frequency of 6 Hz. Reproduced with permission from reference 190. Copyright 2003 Elsevier.

The mesoscale OFR systems have been applied in numerous biological applications for batch and continuous setups.[191-193] Gas-liquid contacting experiments have been performed for mass transfer investigations and up to a 2-fold increase in the k_La values reported for a 50 mm conventional batch OFR were observed.[194,195] Applications in catalysis,[196,197] chemical

synthesis[198] and nanoparticle formation[199,200] have also been reported. Additionally, alternative baffle designs have been investigated[201-203] and some specific advantages have been described for helical-type baffles as these generate a 'swirling flow' in addition to vortices which has potential benefits in terms of heat transfer and encrustation mitigation.[201,204] The helicity is also particularly suited to solid-liquid systems as the design does not feature such pronounced constrictions where particles can become lodged. Interestingly, it has been reported that plug-flow behavior in these systems could be achieved over a much wider range of Re_0 compared to alternative designs,[205,206] see **Figure 14**.

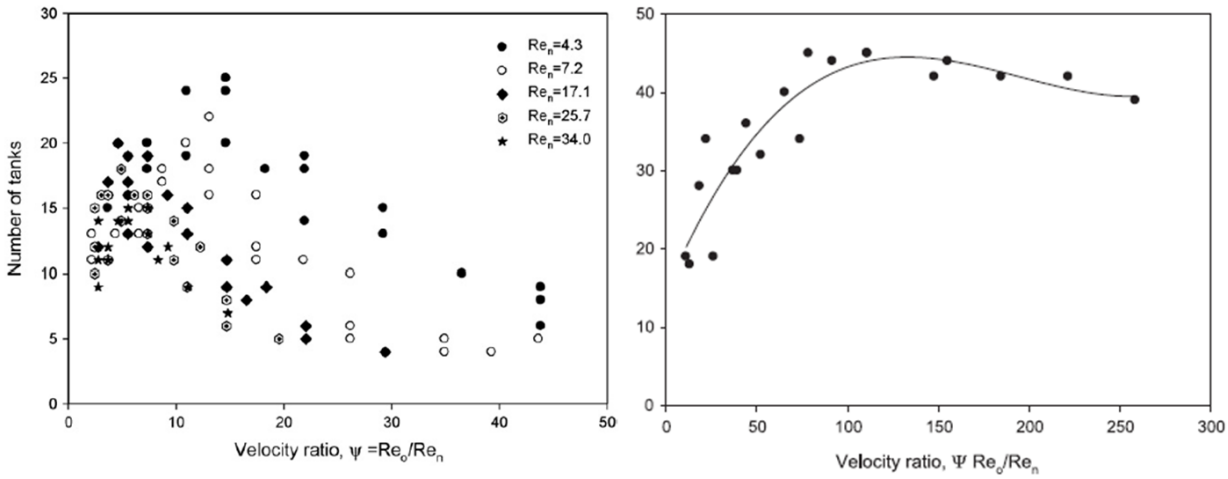

Figure 14. Dependence of RTD performances on velocity ratio (ψ) for a central baffled reactor (left) and a helical baffled reactor (right). Reproduced with permission from references 201 and 205. Copyright 2003 Elsevier.

A summary of the desirable operating conditions for the mesoscale OFR systems is shown below in **Table 4**.

Table 4. Summary of the accepted ranges for Re_0, St, Re_n and ψ for mesoscale COFRs based on the existing literature.

Re_0	St	Re_n	ψ
< 100 (axi-symmetric laminar flow)[187]	0.1 (non axi-symmetric eddies)[117]	< 10 (oscillation conditions have a strong effect on RTD)[201]	>10 (axial dispersion little affected by net flow)[190]
> 100 (flow 3-D, no axi-symmetry, turbulent-like)[187]	0.35 (axi-symmetric eddies),[117] minimum deviation from plug-flow	> 10 (minimal value for convection i.e. sufficient mixing)[117]	4 - 10 (best approximation to plug-flow)[201]
100 - 300 (minimal axial dispersion)[190]	Optimal values with alternative baffle designs[201] including helical[204,205] and low flow rates of 0.3 – 0.6 ml/min[202]	>25 (oscillation conditions have little effect on RTD)[201]	
>300 (minimal effects on axial dispersion)[190]			

Examples of crystallization in OFR platforms

To date there has been various examples in the literature where OFR technology has been applied to crystallization processes. Crystal suspensions are relatively sensitive to mechanical collisions or regions of high shear introduced by impeller blades as these lead to crystal breakage or attrition. This is especially relevant when interested in obtaining crystals with desired particle attributes. The attraction of a COBC, whilst operating at a controlled steady state and under specified de-supersaturation conditions, is that each particle can in theory experience identical conditions during the lifetime in the crystallizer, leading to a uniform and consistent product flow at the end. In addition there are no impellers which can lead to attrition and undesired secondary nucleation. The majority of the existing work has been focused on batch OBC systems, either MF or MB, and comparisons have been made with STC platforms using comparable power density values.

Various crystal systems have been investigated in batch OBC platforms including paracetamol,[86,207,208] LGA[209-211] and sodium chlorate.[101,212,213] These studies (largely cooling

crystallization) have included the effects of strain and shear on crystal suspensions and it is evident that the hydrodynamic environment of oscillatory mixing offers significant advantages, see **Figure 15**. Interestingly, narrower MSZWs were obtained in the MB batch OBC (compared to an STC), most likely due to the mechanical interaction of the baffles and the vessel walls. This effect was also observed using the achiral compound sodium chlorate.[101] The polymorphic nature of LGA has allowed useful studies in batch OBC platforms. In addition, the effects of mixing intensity, seeding and composition of baffle material on LGA crystallization have also been investigated. It has generally been shown that by controlling the process parameters, the desired crystal polymorph could be obtained in the batch OBC.

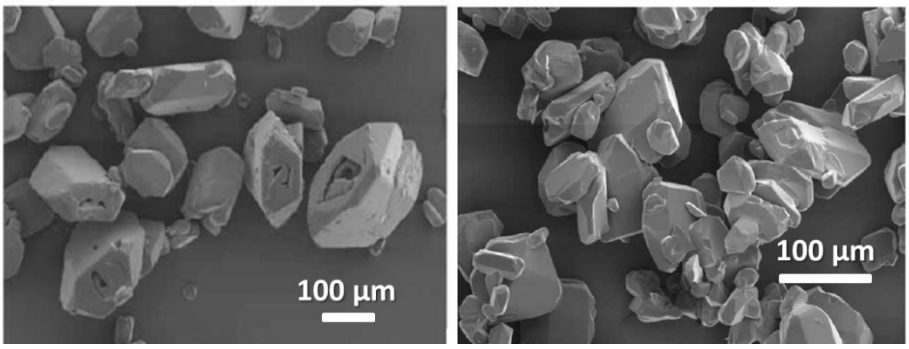

Figure 15. SEM images of paracetamol crystals produced from a batch OBC setup.[208] The OBC (right) has been shown to exhibit a lower strain rate when compared to an STC (left). Reproduced with permission from reference 208. Copyright 2003.

Batch OFRs have traditionally been used as screening platforms prior to continuous experimentation for applications such as polymerization or chemical and biological processing as this allows evaluation at manageable scales. These have also been used to some extent for continuous crystallization evaluation[35,42] however it is important to realize that optimization on such platforms does not fully translate for such application. Nucleation promoting environments such as moving baffles, pistons or bellows may provide potentially misleading information and

this must be taken into consideration. For illustration, we performed a qualitative MSZW study using paracetamol in a water:isopropanol (60:40 wt./wt.) mixture using batch MB and MF OBC platforms. Focused beam reflectance measurement (FBRM), a common, and expensive, in-line monitoring technique for crystallization was used to detect the nucleation temperatures. It was observed that the nucleation induction time for the MB OBC was significantly lower than the MF OBC platform – almost as soon as the supersaturated region was entered, primary nucleation took place, see **Figure 16**.

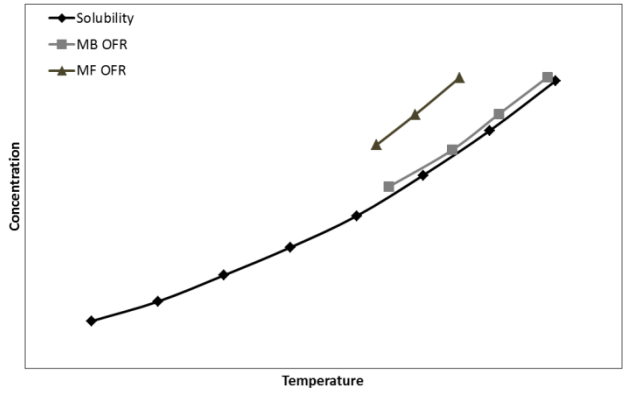

Figure 16. Comparison of MSZWs obtained for MF and MB OBC platforms using a paracetamol/water/isopropanol system.

Overall the measurement of kinetic parameters such as MSZW, primary and secondary nucleation and growth rates in a hydrodynamic environment which differs from intended continuous operation will likely lead to discrepancies. It is important to define which information can be obtained via batch methods in order to reliably inform continuous operation (e.g. solubility, residence time, PAT calibrations) or alternatively development at small scale continuous may be more suitable. To that end, we have developed an automated PAT enabled batch MF OBC system for this purpose, the details of which will be published elsewhere.

MF batch OBCs have previously been applied for the determination of kinetic parameters relevant to crystallization studies. Laser illuminated video (LIV) imaging has been used for observing and quantifying the anti-solvent and cooling crystallization of paracetamol and this allowed determination of growth kinetics non-intrusively.[214-216] The determination of MSZW, CSD and the effects of supersaturation and mixing were examined. It was found that the degree of supersaturation had the most significant effect on the overall growth rates, followed closely by the degree of mixing and then the rate of anti-solvent addition. Both MSZW and mean crystal size were shown to decrease with increasing Re_0 and it was demonstrated that the LIV technique was as sensitive to nucleation events as FBRM. Very recently, the nucleation kinetics for the cooling crystallization of adipic acid were investigated using Nývlt,[217] Kubota[218] and population balance interpretations.[219] Due to their linear assumptions, both the Nývlt and the Kubota interpretations were found to be most accurate over a narrower range of cooling rates, whereas the nonlinear nature of the population balance approach makes it accurate over a much wider range.

The OBC has also been applied for continuous crystallization, see **Figure 17**. Ni demonstrated successful crystallization of a model API in a glass COBC of length 25 m (d = 25 mm) with a residence time of 12 min compared to a 9.5 h batch process.[35] Recently we used a 25 m (d = 15 mm) glass COBC for the scale-up of a novel α-lipoic acid:nicotinamide co-crystal system.[42] The use a glass COBC (d = 15 mm) for the anti-solvent crystallization of salicylic acid with solute concentration steady states maintained for >100 residence times has also been demonstrated.[54] Extended operation for 6.25 h allowed the generation of *ca.* 1 kg of product material. While the successful operation of these processes is highly encouraging for the application of continuous crystallization, further research and development is still required for moving towards feasible

implementation in industrial applications. Increased automation, PAT and real-time feedback control are important considerations under current investigation. It is also important to consider the integration of continuous crystallization with other unit operations both up- and downstream.

Figure 17. Images of laboratory COBC systems.

One of the most important challenges associated with the operation of COBCs and also of general reference to continuous crystallization itself is encrustation, see **Figure 18**. This manifests itself as an unpredictable solid formation at internal equipment walls causing disruption to steady state operation which can cause interference with heat transfer or PAT measurements or even cause complete blockage of the system. Encrustation can be the result of specific interactions between a given surface and molecule in addition to solvent dependency or be the result of poor control of supersaturation. The generation of high levels of supersaturation substantially beyond solubility will likely lead to nucleation on a surface as opposed to the bulk. Physical mitigation approaches to encrustation have been reported including ultrasound,[52] surface coatings[220] and additives[221] however crystal engineering strategies such as seeding, temperature cycling or controlling primary nucleation via external intervention such as ultrasound or laser induced nucleation may also be effective. Nagy *et al.*[222] recently proposed a mitigation strategy that relies on injection of pure solvent to dissolve an encrusted layer in a

continuous plug-flow crystallizer. Significant issues with encrustation should be flagged up early during process design via batch evaluation or small scale continuous operation. If the problem is not feasibly resolvable, this should inform the decision in considering a specific continuous platform such as a COBC.

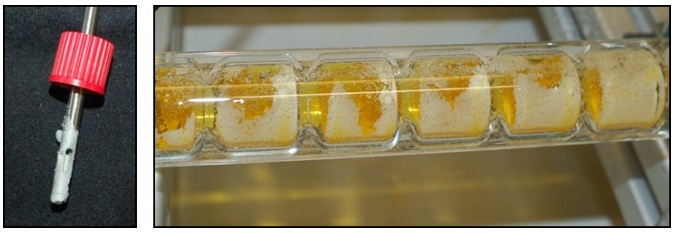

Figure 18. Images highlighting encrustation. Left: a PAT probe and right: a tubular section of a COBC.

We specifically operated a continuously seeded crystallization process for LGA in a 25 m glass COBC system (d = 15 mm).[223] Attempting to operate the process without seeding led to significant encrustation such that the crystallizer had to be shut down. However, by seeding with β-LGA crystals and maintaining a bulk supersaturation below 3, the polymorphic phase purity of the thermodynamically stable β-polymorph was retained allowing robust processing for at least 10 hours. Additionally, we performed a continuously seeded sonocrystallization of alpha-lactose monohydrate in a 3.5 m, multi-orifice, polished stainless steel COBC (d_e = 69 mm).[224] This allowed a throughput of 356 g h^{-1} for 12 - 16 hours operation. Kinetic and thermodynamic parameters were evaluated in a batch evaluation unit which provided a suitable mimic of the mixing, hydrodynamics and operating conditions of the continuous platform whilst consuming limited material. PAT including FBRM and mid-IR was implemented in both batch and continuous experimentation in order to understand and monitor the process.

For both of these studies, continuous seeding was essential in allowing robust operation with no evidence of encrustation leading to process disruption. As a result, suitable strategies for the generation of seed streams must be considered in order to feed into the subsequent growth process. We have developed a novel continuous anti-solvent nucleation unit which has been used to produce paracetamol seed crystals with a narrow size distribution.[225] The nucleation unit operated at sufficiently high supersaturations and could be used to produce seed crystals with a high degree of reproducibility.

An overall summary of the use of OBC technology for crystallization is shown below in **Table 5**.

Table 5. Summary of crystallization applications for the OBC system.

System	Technique	Batch / Continuous	Year	Conclusion	Reference
paracetamol	Cooling	Batch	2004, 2005, 2007	Improved crystal quality (CSD, surface, microstrain)	Ristic[86,207,208]
L-glutamic acid	Cooling, seeding	Batch	2004, 2008, 2009	Polymorph control, OBC promotes nucleation hence reduces MSZW, baffle MOC effects	Ni,[209,210] Roberts[211]
Astrazeneca API	Cooling	Batch and Continuous	2009	Batch: faster cooling rates possible leading to desired crystal habit, improved CSDs. Continuous: residence time reduced from 9.5 h to 12 min	Ni[35]
paracetamol	Cooling, anti-solvent	Batch	2011	Laser illuminated video imaging used non-intrusively to evaluate MSZW, growth rates, CSD, mean crystal size	Ni[214-216]
sodium chlorate	Cooling, seeding	Batch	2012, 2014	Moving baffles promote unexpected nucleation of opposite enantiomer to seeding species	Ni[101,212]

α-lipoic acid: nicotinamide co-crystal	Cooling	Batch and Continuous	2014	Successful scale-up of unique co-crystal system in COBC	Florence[42]
Adipic acid	Cooling	Batch	2014	Evaluation of crystallization kinetics	Ni[219]
Salicylic acid	Anti-solvent	Continuous	2015	Extended operation for 6.25 h (>100 residence times), 1 kg product	Ni[54]
Lactose	Cooling	Continuous	2015	Sonocrystallization, use of batch evaluation platform to design continuous, PAT monitoring	Florence[224]
L-glutamic acid	Cooling	Continuous	2015	Encrustation mitigation by continuous seeding, polymorph control	Florence[223]

Future and outlook

This review aimed to provide a fairly comprehensive summary of OFR characterization, operation and application in the literature with a view that such systems are promising platforms for continuous crystallization. Historically, the application of oscillatory mixing has shown marked benefits in terms of heat and mass transfer resulting in improvements in chemical reaction, polymerization and catalysis. The concept of a continuous, plug-flow platform with relatively low flow rate is highly appealing for crystallization. The complex nature of the process (nucleation, growth, attrition etc) results in notable challenges for traditional batch processing . Continuous and controlled steady state operation may provide the required conditions to allow control of CSD, polymorphism, impurities etc in a highly reproducible manner.

A comprehensive and validated workflow is required for the successful delivery of a continuous crystallization process. This will allow such a campaign to be broken into stages, with decision points at each informing the subsequent actions. Much of the development work can be completed in batch type setups but care should be taken regarding optimization of kinetic

parameters such as nucleation for example as this will do little to predict behavior in a continuous environment. The workflow will also allow informed decisions to be made regarding the feasibility of continuous operation as this will not be suitable for each and every case.

The scaling down of COFRs is particularly timely with regards to lab-scale development and operation. Traditional COFR platforms required a significant commitment in terms of materials in addition to human resource for operation. As there are challenges in simulating the hydrodynamic environment of continuous in batch-type setups, the level of development still required at the continuous stage is too high. The mesoscale COFR systems are showing significant promise as lab-scale continuous crystallizers however there remain the issues of high solid loadings and encrustation. Characterization of these platforms is critical, specifically in terms of CFD and RTD. Whilst good progress has been made to date, an important challenge will be characterization combining both the solid and liquid phases associated with crystallization. The application of image processing will be critical in tackling this important challenge. In general, the future benefits of continuous crystallization are likely to lie in a comprised situation between mesoscale and traditional operation and scaling up may be less of interest when compared to parallelization and longer operation times.

Materials of construction are additionally an interesting topic associated with COFRs. Permanent glass and metal based platforms result in a lack of flexibility and substantial cleaning protocols between campaigns. Polymer-based disposable reactors may provide some solutions towards tackling these issues.

Professor Alastair Florence

*E-mail: alastair.florence@strath.ac.uk; Fax: +44 (0)141 552 2562; Tel: +44 (0)141 548 4877

Author Contributions

The manuscript was written through contributions of all authors. All authors have given approval to the final version of the manuscript.

Funding Sources

We would like to acknowledge the EPSRC Centre for Innovative Manufacturing in Continuous Manufacturing and Crystallisation for funding.

ABBREVIATIONS

API	Active pharmaceutical ingredient
ATR	Agitated tube reactor
CFD	Computational fluid dynamics
CM	Continuous manufacturing
COBC	Continuous oscillatory baffled crystalliser
COBR	Continuous oscillatory baffled reactor
COFR	Continuous oscillatory flow reactor
CQA	Critical quality attribute
CSD	Crystal size distribution
CSTR	Continuous stirred tank reactor
DSD	Droplet size distribution
EIT	Electrical impedance tomography
FBRM	Focused beam reflectance measurement
HAp	Hydroxyapatite
LES	Large eddy simulation
LGA	*L*-glutamic acid
LIF	Laser induced fluorescence
LIV	Laser illuminated video
MB	Moving baffle
MF	Moving fluid
MSMPR	Mixed suspension mixed product removal
MSZW	Metastable zone width
OBC	Oscillatory baffled crystalliser
OBCl	Oscillatory baffled column
OBR	Oscillatory baffled reactor
OFR	Oscillatory flow reactor
PAT	Process analytical technology
PBM	Population balance modelling

PFR	Plug-flow reactor
PuFR	Pulsed-flow reactor
PIV	Particle image velocimetry
PPC	Pulsed pack column
PTC	Phase transfer catalysis
QbD	Quality by design
RPC	Reciprocating plate column
RTD	Residence time distribution
SPC	Smooth periodic constriction
STC	Stirred tank crystalliser
STFR	Segmented tube flow reactor
STR	Stirred tank reactor

NOMENCLATURE

c	solution concentration, kg l^{-1}
C_D	discharge coefficient of the baffles
d	tube inner diameter, m
d_e	effective tube diameter, m
d_0	baffle orifice diameter, m
D	axial dispersion coefficient, m^2 s^{-1}
D_{imp}	impeller diameter, m
f	oscillation frequency, Hz
h_t	tube-side heat transfer coefficient
k	thermal conductivity of the fluid
k_L	liquid-side mass transfer coefficient
k_La	volumetric mass transfer coefficient
l	length, m
l_e	Mixing length for eddy enhancement model
L	baffle spacing, m
n	number of tanks in series
n_o	number of orifices
N	impeller speed, s^{-1}
N_b	number of baffles per unit length of tube
Nu	tube-side Nusselt number
P/V	power density, W m^{-3}
P_0	power number
Q	flow rate, m^3 min^{-1}

R_V	ratio of the plane-averaged axial over the radial velocity
Re	Reynolds number
Re_n	net flow Reynolds number
Re_0	oscillatory Reynolds number
Re_{pipe}	Reynolds number for flow through a tube
Re_{STR}	Reynolds number for a stirred tank reactor
St	Strouhal number
t	time, s
u	superficial net flow velocity, m s^{-1}
V_L	volume of liquid in STC
x	position along axial length, m
x_0	oscillation amplitude (centre-to-peak), m

Greek symbols

α	baffle orifice/tube cross sectional area ratio
δ	baffle thickness, m
η	stage-wise efficiency term
ρ	fluid density, kg m^{-3}
τ	residence time, min
μ	fluid viscosity, kg m^{-1} s^{-1}
ν	kinematic viscosity, m^2 s^{-1}
ψ	velocity ratio

REFERENCES

(1) Schaber, S. D.; Gerogiorgis, D. I.; Ramachandran, R.; Evans, J. M. B.; Barton, P. I.; Trout, B. L. *Ind Eng Chem Res* **2011**, *50*, 10083.
(2) Baxendale, I. R. *J Chem Technol Biot* **2013**, *88*, 519.
(3) Hartman, R. L.; McMullen, J. P.; Jensen, K. F. *Angew Chem Int Edit* **2011**, *50*, 7502.
(4) Hessel, V.; Kralisch, D.; Kockmann, N.; Noel, T.; Wang, Q. *Chemsuschem* **2013**, *6*, 746.
(5) Webb, D.; Jamison, T. F. *Chem Sci* **2010**, *1*, 675.
(6) Singh, B.; Rizvi, S. S. H. *J Dairy Sci* **1994**, *77*, 3809.
(7) Yu, Z. Q.; Lv, Y. W.; Yu, C. M. *Org Process Res Dev* **2012**, *16*, 1669.
(8) Anastas, P. T.; Zimmerman, J. B. *Sustain Sci Eng* **2006**, *1*, 11.
(9) Yoshida, J. I.; Kim, H.; Nagaki, A. *Chemsuschem* **2011**, *4*, 331.
(10) Anderson, N. G. *Org Process Res Dev* **2012**, *16*, 852.
(11) Leuenberger, H. *Eur J Pharm Biopharm* **2001**, *52*, 289.

(12) Bogaert-Alvarez, R. J.; Demena, P.; Kodersha, G.; Polomski, R. E.; Soundararajan, N.; Wang, S. S. Y. *Org Process Res Dev* **2001**, *5*, 636.
(13) LaPorte, T. L.; Hamedi, M.; DePue, J. S.; Shen, L. F.; Watson, D.; Hsieh, D. *Org Process Res Dev* **2008**, *12*, 956.
(14) Baxendale, I. R.; Braatz, R. D.; Hodnett, B. K.; Jensen, K. F.; Johnson, M. D.; Sharratt, P.; Sherlock, J. P.; Florence, A. J. *J Pharm Sci-Us* **2015**, *104*, 781.
(15) Plumb, K. *Chem Eng Res Des* **2005**, *83*, 730.
(16) Whitesides, G. M. *Nature* **2006**, *442*, 368.
(17) Mason, B. P.; Price, K. E.; Steinbacher, J. L.; Bogdan, A. R.; McQuade, D. T. *Chem Rev* **2007**, *107*, 2300.
(18) Wegner, J.; Ceylan, S.; Kirschning, A. *Chem Commun* **2011**, *47*, 4583.
(19) Mascia, S.; Heider, P. L.; Zhang, H. T.; Lakerveld, R.; Benyahia, B.; Barton, P. I.; Braatz, R. D.; Cooney, C. L.; Evans, J. M. B.; Jamison, T. F.; Jensen, K. F.; Myerson, A. S.; Trout, B. L. *Angew Chem Int Edit* **2013**, *52*, 12359.
(20) Heider, P. L.; Born, S. C.; Basak, S.; Benyahia, B.; Lakerveld, R.; Zhang, H. T.; Hogan, R.; Buchbinder, L.; Wolfe, A.; Mascia, S.; Evans, J. M. B.; Jamison, T. F.; Jensen, K. F. *Org Process Res Dev* **2014**, *18*, 402.
(21) Zhang, H. T.; Lakerveld, R.; Heider, P. L.; Tao, M. Y.; Su, M.; Testa, C. J.; D'Antonio, A. N.; Barton, P. I.; Braatz, R. D.; Trout, B. L.; Myerson, A. S.; Jensen, K. F.; Evans, J. M. B. *Cryst Growth Des* **2014**, *14*, 2148.
(22) Bermingham, S. K.; Neumann, A. M.; Kramer, H. J. M.; Verheijen, P. J. T.; van Rosmalen, G. M.; Grievink, J. *Aiche Sym S* **2000**, *96*, 250.
(23) Srai, J. S.; Gregory, M. *Int J Oper Prod Man* **2008**, *28*, 386.
(24) Pesti, J. A. *Org Process Res Dev* **2014**, *18*, 1284.
(25) Chen, J.; Sarma, B.; Evans, J. M. B.; Myerson, A. S. *Cryst Growth Des* **2011**, *11*, 887.
(26) Mullin, J. W. *Crystallisation*; 4th ed. Oxford, 2001.
(27) Barrett, P.; Glennon, B. *Chem Eng Res Des* **2002**, *80*, 799.
(28) Saleemi, A.; Rielly, C.; Nagy, Z. K. *Crystengcomm* **2012**, *14*, 2196.
(29) Khaddour, I.; Rocha, F. *Cryst Res Technol* **2011**, *46*, 373.
(30) Yu, L. X. *Pharm Res-Dordr* **2008**, *25*, 2463.
(31) Eder, R. J. P.; Radl, S.; Schmitt, E.; Innerhofer, S.; Maier, M.; Gruber-Woelfler, H.; Khinast, J. G. *Cryst Growth Des* **2010**, *10*, 2247.
(32) Myerson, A. S.; Krumme, M.; Nasr, M.; Thomas, H.; Braatz, R. D. *J Pharm Sci-Us* **2015**, *104*, 832.
(33) Yang, Y.; Nagy, Z. K. *Ind Eng Chem Res* **2015**, *54*, 5673.
(34) Variankaval, N.; Cote, A. S.; Doherty, M. F. *Aiche J* **2008**, *54*, 1682.
(35) Lawton, S.; Steele, G.; Shering, P.; Zhao, L. H.; Laird, I.; Ni, X. W. *Org Process Res Dev* **2009**, *13*, 1357.
(36) Levenspiel, O. *Chemical Reaction Engineering* 3rd ed.; Wiley: New York, USA, 1999.
(37) Neugebauer, P.; Khinast, J. G. *Cryst Growth Des* **2015**, *15*, 1089.
(38) Su, Q. L.; Nagy, Z. K.; Rielly, C. D. *Chem Eng Process* **2015**, *89*, 41.
(39) Tavare, N. S. *Aiche J* **1986**, *32*, 705.
(40) Cichy, B.; Kuzdzal, E. *Ind Eng Chem Res* **2014**, *53*, 6593.
(41) Quon, J. L.; Zhang, H.; Alvarez, A.; Evans, J.; Myerson, A. S.; Trout, B. L. *Cryst Growth Des* **2012**, *12*, 3036.

(42) Zhao, L. H.; Raval, V.; Briggs, N. E. B.; Bhardwaj, R. M.; McGlone, T.; Oswald, I. D. H.; Florence, A. J. *Crystengcomm* **2014**, *16*, 5769.
(43) Hou, G. Y.; Power, G.; Barrett, M.; Glennon, B.; Morris, G.; Zhao, Y. *Cryst Growth Des* **2014**, *14*, 1782.
(44) Alvarez, A. J.; Singh, A.; Myerson, A. S. *Cryst Growth Des* **2011**, *11*, 4392.
(45) Kozik, A.; Hutnik, N.; Piotrowski, K.; Matynia, A. *Chem Eng Res Des* **2014**, *92*, 481.
(46) Zhang, H. T.; Quon, J.; Alvarez, A. J.; Evans, J.; Myerson, A. S.; Trout, B. *Org Process Res Dev* **2012**, *16*, 915.
(47) Alvarez, A. J.; Myerson, A. S. *Cryst Growth Des* **2010**, *10*, 2219.
(48) Gerard, A.; Muhr, H.; Plasari, E.; Jacob, D.; Lefaucheur, C. E. *Powder Technol* **2014**, *255*, 134.
(49) Vacassy, R.; Lemaitre, J.; Hofmann, H.; Gerlings, J. H. *Aiche J* **2000**, *46*, 1241.
(50) Ferguson, S.; Ortner, F.; Quon, J.; Peeva, L.; Livingston, A.; Trout, B. L.; Myerson, A. S. *Cryst Growth Des* **2014**, *14*, 617.
(51) Ferguson, S.; Morris, G.; Hao, H. X.; Barrett, M.; Glennon, B. *Chem Eng Sci* **2013**, *104*, 44.
(52) Eder, R. J. P.; Schrank, S.; Besenhard, M. O.; Roblegg, E.; Gruber-Woelfler, H.; Khinast, J. G. *Cryst Growth Des* **2012**, *12*, 4733.
(53) Narducci, O.; Jones, A. G.; Kougoulos, E. *Chem Eng Sci* **2011**, *66*, 1069.
(54) Brown, C. J. Adelakun, J. A.; Ni, X. *Chem Eng Process: Process Intensification* **2015**, *Advance article: doi:10.1016/j.cep.2015.04.012*.
(55) Wong, S. Y.; Tatusko, A. P.; Trout, B. L.; Myerson, A. S. *Cryst Growth Des* **2012**, *12*, 5701.
(56) Wierzbowska, B.; Piotrowski, K.; Koralewska, J.; Matynia, A.; Hutnik, N.; Wawrzyniecki, K. *Cryst Res Technol* **2008**, *43*, 381.
(57) Wong, S. Y.; Bund, R. K.; Connelly, R. K.; Hartel, R. W. *Cryst Growth Des* **2010**, *10*, 2620.
(58) de Paz, G. D. *Int Sugar J* **2002**, *104*, 14.(59) Wojcik, J. A.; Jones, A. G. *Chem Eng Res Des* **1997**, *75*, 113.
(60) Lai, T.-T. C. F., S.; Palmer, L.; Trout, B. L.; Myerson, A. S. *Org Process Res Dev* **2014**, *18,* 1382.
(61) Tai, C. Y.; Shei, W. L. *Chem Eng Commun* **1993**, *120*, 139.
(62) Jones, A. G.; Mydlarz, J. *Chem Eng Res Des* **1989**, *67*, 283.
(63) Abbott, M. S. R.; Harvey, A. P.; Perez, G. V.; Theodorou, M. K. *Interface Focus* **2013**, *3*.
(64) Mackley, M. R. *Chem Eng Res Des* **1991**, *69*, 197.
(65) Ni, X.; Mackley, M. R.; Harvey, A. P.; Stonestreet, P.; Baird, M. H. I.; Rao, N. V. R. *Chem Eng Res Des* **2003**, *81*, 373.
(66) Stonestreet, P.; Harvey, A. P. *Chem Eng Res Des* **2002**, *80*, 31.
(67) Nogueira, X.; Taylor, B. J.; Gomez, H.; Colominas, I.; Mackley, M. R. *Comput Chem Eng* **2013**, *49*, 1.
(68) Harji, B. Crystallisation process and apparatus (Patent, WO 2011/051728 A1) **2010**
(69) Gough, P.; Ni, X. W.; Symes, K. C. *J Chem Technol Biot* **1997**, *69*, 321.
(70) Mackley, M. R.; Stonestreet, P. *Chem Eng Sci* **1995**, *50*, 2211.
(71) Mackley, M. R.; Tweddle, G. M.; Wyatt, I. D. *Chem Eng Sci* **1990**, *45*, 1237.
(72) Hewgill, M. R.; Mackley, M. R.; Pandit, A. B.; Pannu, S. S. *Chem Eng Sci* **1993**, *48*, 799.
(73) Ni, X.; Gao, S.; Cumming, R. H.; Pritchard, D. W. *Chem Eng Sci* **1995**, *50*, 2127.

(74) Ni, X. W.; Gao, S. W.; Pritchard, D. W. *Biotechnol Bioeng* **1995**, *45*, 165.
(75) Mackley, M. R.; Smith, K. B.; Wise, N. P. *Chem Eng Res Des* **1993**, *71*, 649.
(76) Ni, X.; Mackley, M. R. *Chem Eng J Bioch Eng* **1993**, *52*, 107.
(77) Ni, X.; Zhang, Y.; Mustafa, I. *Chem Eng Sci* **1998**, *53*, 2903.
(78) Ni, X.; Zhang, Y.; Mustafa, I. *Chem Eng Sci* **1999**, *54*, 841.
(79) Gao, S. N., X.; Cumming, R. H.; Greated, C. A.; Norman, P. *Separation Sci Tech* **1998**, *33(14)*, 2143.
(80) Brunold, C. R.; Hunns, J. C. B.; Mackley, M. R.; Thompson, J. W. *Chem Eng Sci* **1989**, *44*, 1227.
(81) Mackley, M. R.; Ni, X. *Chem Eng Sci* **1991**, *46*, 3139.
(82) Mackley, M. R.; Ni, X. *Chem Eng Sci* **1993**, *48*, 3293.
(83) Ni, X. L., S.; Grewal, P. S.; Greated, C. A. *J Flow Visualisation & Image Process* **1995**, *2*, 135.
(84) Dickens, A. W.; Mackley, M. R.; Williams, H. R. *Chem Eng Sci* **1989**, *44*, 1471.
(85) Ni, X. W. *J Chem Technol Biot* **1994**, *59*, 213.
(86) Chew, C. M.; Ristic, R. I. *Aiche J* **2005**, *51*, 1576.
(87) Howes, T. **1988**, *PhD Thesis, Dept. Chem. Eng., Cambridge University, On the dispersion of unsteady flow in baffled tubes*
(88) Howes, T.; Mackley, M. R. *Chem Eng Sci* **1990**, *45*, 1349.
(89) Liu, S.; Ni, X.; Greated, C. A.; Fryer, P. J. *Chem Eng Res Des* **1995**, *73*, 727.
(90) Ni, X.; Gao, S. *Chem Eng J* **1996**, *63*, 157.
(91) Jongen, N.; Donnet, M.; Bowen, P.; Lemaitre, J.; Hofmann, H.; Schenk, R.; Hofmann, C.; Aoun-Habbache, M.; Guillemet-Fritsch, S.; Sarrias, J.; Rousset, A.; Viviani, M.; Buscaglia, M. T.; Buscaglia, V.; Nanni, P.; Testino, A.; Herguijuela, J. R. *Chem Eng Technol* **2003**, *26*, 303.
(92) Gasparini, G.; Archer, I.; Jones, E.; Ashe, R. *Org Process Res Dev* **2012**, *16*, 1013.
(93) Van Dick, W. J. D. Process and apparatus for intimately contacting fluids (Patent US 2,011,186) **1935**.
(94) Baird, M. H. I.; Rao, N. V. R. *Can J Chem Eng* **1995**, *73*, 417.
(95) Baird, M. H. I. R. R., N. V.; Prochazka, J.; Sovova, H. *Reciprocating plate columns in solvent extraction equipment design*; Wiley: Chichester UK, 1994.
(96) Baird, M. H. I.; Garstang, J. H. *Chem Eng Sci* **1972**, *27*, 823.
(97) Godfrey, J. C. S., M. J. *Liquid-liquid extraction equipment*; John Wiley: New York, USA, 1994.
(98) Lo, T. C. B., M. H. I.; Hanson, C. *Handbook of solvent extraction*; John Wiley & Sons: New York, USA, 1983.
(99) Mak, A. N. S.; Koning, C. A. J.; Hamersma, P. J.; Fortuin, J. M. H. *Chem Eng Sci* **1991**, *46*, 819.
(100) Baird, M. H. I.; Rao, N. V. R. *Can J Chem Eng* **1988**, *66*, 222.
(101) Callahan, C. J.; Ni, X. W. *Cryst Growth Des* **2012**, *12*, 2525.
(102) Prochazka, J. R., V. Apparatus for Bringing Fluid Phases into Mutual Contact (Patent, US 3,855,368) **1974**.
(103) Skala, D.; Veljkovic, V. *Can J Chem Eng* **1988**, *66*, 192.
(104) Hounslow, M. J.; Ni, X. *Chem Eng Sci* **2004**, *59*, 819.
(105) Harrison, S. T. L.; Mackley, M. R. *Chem Eng Sci* **1992**, *47*, 490.
(106) Simon, L. L. e. a. *Org Process Res Dev* **2015**, *19*, 3

(107) McDonough, J. R. P., A. N.; Harvey, A. P. *Chem Eng J* **2015**, *265*, 110
(108) Reis, N. M. F. **2006**, *PhD Thesis, School of Engineering, University of Minho, Portugal, Novel oscillatory flow reactors for biotechnological applications*.
(109) Smith, K. B. **1999**, *PhD Thesis,Christ's College, Cambridge, The scale-up of oscillatory flow mixing*.
(110) Majumder, A.; Nagy, Z. K. *Aiche J* **2013**, *59*, 4582.
(111) Ridder, B. J.; Majumder, A.; Nagy, Z. K. *Ind Eng Chem Res* **2014**, *53*, 4387.
(112) Vetter, T.; Burcham, C. L.; Doherty, M. F. *Chem Eng Sci* **2014**, *106*, 167.
(113) Ni, X. W.; Nelson, G.; Mustafa, I. *Can J Chem Eng* **2000**, *78*, 211.
(114) Zhang, Y. M.; Ni, X. W.; Mustafa, I. *J Chem Technol Biot* **1996**, *66*, 305.
(115) Ferreira, A.; Teixeira, J. A.; Rocha, F. *Chem Eng J* **2015**, *262*, 499.
(116) Pereira, F. M.; Sousa, D. Z.; Alves, M. M.; Mackley, M. R.; Reis, N. M. *Ind Eng Chem Res* **2014**, *53*, 17303.
(117) Harvey, A. P. M., M. R.; Reis, N.; Vicente, A. A.; Teixeira, J. A. *4th European Congress of Chemical Engineering, Granada, pp. 0-6.4-004* **2003**.
(118) Knott, G. F.; Mackley, M. R. *Philos T R Soc A* **1980**, *294*, 599.
(119) Mackley, M. *J Chem Technol Biot* **2003**, *78*, 94.
(120) Ni, X.; Brogan, G.; Struthers, A.; Bennett, D. C.; Wilson, S. F. *Chem Eng Res Des* **1998**, *76*, 635.
(121) Ni, X.; Gough, P. *Chem Eng Sci* **1997**, *52*, 3209.
(122) Nishimura, T.; Ohori, Y.; Kajimoto, Y.; Kawamura, Y. *J Chem Eng Jpn* **1985**, *18*, 550.
(123) Sobey, I. J. *J Fluid Mech* **1980**, *96*, 1.
(124) Sobey, I. J. *J Fluid Mech* **1985**, *151*, 395.
(125) Stonestreet, P.; Van der Veeken, P. M. J. *Chem Eng Res Des* **1999**, *77*, 671.
(126) Ni, X. W.; de Gelicourt, Y. S.; Neil, J.; Howes, T. *Chem Eng J* **2002**, *85*, 17.
(127) Takriff, M. S.; Masyithah, Z. *Chem Eng Commun* **2002**, *189*, 1640.
(128) Nienow, A. W.; Miles, D. *Ind Eng Chem Proc Dd* **1971**, *10*, 41.
(129) Jealous, A. C.; Johnson, H. F. *Ind Eng Chem* **1955**, *47*, 1168.
(130) Baird, M. H. I.; Stonestreet, P. *Chem Eng Res Des* **1995**, *73*, 503.
(131) Baird, M. H. I.; Garstang, J. H. *Chem Eng Sci* **1967**, *22*, 1663.
(132) Stephens, G. G.; Mackley, M. R. *Exp Therm Fluid Sci* **2002**, *25*, 583.
(133) Mackley, M. R.; Stonestreet, P.; Thurston, N. C.; Wiseman, J. S. *Can J Chem Eng* **1998**, *76*, 5.
(134) Oliveira, M. S. N.; Ni, X. *Chem Eng Sci* **2001**, *56*, 6143.
(135) Oliveira, M. S. N.; Ni, X. W. *Chem Eng J* **2004**, *99*, 59.
(136) Lau, A.; Crittenden, B. D.; Field, R. W. *Sep Purif Technol* **2004**, *35*, 113.
(137) Ni, X. W.; Gao, S. W.; Santangeli, L. *J Chem Technol Biot* **1997**, *69*, 247.
(138) Jones, E. H.; Bajura, R. A. *J Fluid Eng-T Asme* **1991**, *113*, 199.
(139) Ralph, M. E. *J Fluid Mech* **1986**, *168*, 515.
(140) Sobey, I. J. *J Fluid Mech* **1983**, *134*, 247.
(141) E. P. L. Roberts, E. P. L. **1992**, *PhD Thesis, Cambridge, Unsteady flow and mixing in baffled channels*.
(142) Roberts, E. P. L.; Mackley, M. R. *Chem Eng Sci* **1995**, *50*, 3727.
(143) Chew, C. M.; Ristic, R. I.; Reynolds, G. K.; Ooi, R. C. *Chem Eng Sci* **2004**, *59*, 1557.
(144) Ni, X.; Jian, H.; Fitch, A. *Chem Eng Res Des* **2003**, *81*, 842.

(145) Hamzah, A. A.; Hasan, N.; Takriff, M. S.; Kamarudin, S. K.; Abdullah, J.; Tan, I. M.; Sern, W. K. *Chem Eng Res Des* **2012**, *90*, 1038.
(146) Jian, H. B.; Ni, X. W. *J Chem Technol Biot* **2003**, *78*, 321.
(147) Ni, X.; Jian, H.; Fitch, A. W. *Chem Eng Sci* **2002**, *57*, 2849.
(148) Roberts, E. P. L.; Mackley, M. R. *J Fluid Mech* **1996**, *328*, 19.
(149) Zheng, M. Z.; Li, J.; Mackley, M. R.; Tao, J. J. *Phys Fluids* **2007**, *19*, 114101
(150) Fitch, A. W.; Jian, H. B.; Ni, X. W. *Chem Eng J* **2005**, *112*, 197.
(151) Mackley, M. R.; Saraiva, R. M. C. N. *Chem Eng Sci* **1999**, *54*, 159.
(152) Howes, T.; Mackley, M. R.; Roberts, E. P. L. *Chem Eng Sci* **1991**, *46*, 1669.
(153) Mackay, M. E.; Mackley, M. R.; Wang, Y. *Chem Eng Res Des* **1991**, *69*, 506.
(154) Roberts, E. P. L. *J Fluid Mech* **1994**, *260*, 185.
(155) Manninen, M.; Gorshkova, E.; Immonen, K.; Ni, X. W. *J Chem Technol Biot* **2013**, *88*, 553.
(156) Jian, H.; Ni, X. *Chem Eng Res Des* **2005**, *83*, 1163.
(157) Ni, X.; Cosgrove, J. A.; Arnott, A. D.; Greated, C. A.; Cumming, R. H. *Chem Eng Sci* **2000**, *55*, 3195.
(158) Palma, M.; Giudici, R. *Chem Eng J* **2003**, *94*, 189.
(159) Mackley, M. R.; Stonestreet, P.; Roberts, E. P. L.; Ni, X. *Chem Eng Res Des* **1996**, *74*, 541.
(160) Abbott, M. S. R.; Harvey, A. P.; Morrison, M. I. *Int J Chem React Eng* **2014**, *12*.
(161) Ni, X. W. *J Chem Technol Biot* **1995**, *64*, 165.
(162) Ni, X. W.; Pereira, N. E. *Aiche J* **2000**, *46*, 37.
(163) Fitch, A. W.; Ni, X. *Chem Eng J* **2003**, *92*, 243.
(164) Briggs, N. E. B. **2015**, *PhD Thesis, University of Strathclyde, Glasgow, Polymorph control of pharmaceuticals within a COBC*.
(165) Abbott, M. S. R. P., G. V.; Harvey, A. P.; Theodorou, M. K. *Chem Eng Res Des* **2014**, *90*, 1969
(166) Lee, C. T.; Buswell, A. M.; Middelberg, A. P. J. *Chem Eng Sci* **2002**, *57*, 1679.
(167) Ni, X.; Johnstone, J. C.; Symes, K. C.; Grey, B. D.; Bennett, D. C. *Aiche J* **2001**, *47*, 1746.
(168) Ni, X. W.; Murray, K. R.; Zhang, Y. M.; Bennett, D.; Howes, T. *Powder Technol* **2002**, *124*, 281.
(169) Fabiyi, M. E.; Skelton, R. L. *J Photoch Photobio A* **1999**, *129*, 17.
(170) Fabiyi, M. E.; Skelton, R. L. *J Photoch Photobio A* **2000**, *132*, 121.
(171) Gao, P.; Ching, W. H.; Herrmann, M.; Chan, C. K.; Yue, P. L. *Chem Eng Sci* **2003**, *58*, 1013.
(172) Ni, X.; Cosgrove, J. A.; Cumming, R. H.; Greated, C. A.; Murray, K. R.; Norman, P. *Chem Eng Res Des* **2001**, *79*, 33.
(173) Oliveira, M. S. N.; Ni, X. W. *Aiche J* **2004**, *50*, 3019.
(174) Wilson, B.; Sherrington, D. C.; Ni, X. *Ind Eng Chem Res* **2005**, *44*, 8663.
(175) Brown, C. J.; Ni, X. *Chem Eng J* **2010**, *157*, 131.
(176) Ismail, L.; Westacott, R. E.; Ni, X. W. *J Chem Technol Biot* **2006**, *81*, 1905.
(177) Masngut, N. H., A. P. *Procedia Eng* **2012**, *42*, 1079.
(178) Melendi, S.; Bonyadi, S.; Castell, P.; Martinez, M. T.; Mackley, M. R. *Chem Eng Sci* **2012**, *84*, 544.
(179) Pereira, N. E.; Ni, X. W. *Chem Eng Sci* **2001**, *56*, 735.

(180) Mignard, D.; Amin, L. P.; Ni, X. W. *Chem Eng Sci* **2006**, *61*, 6902.
(181) Ni, X.; Mignard, D.; Saye, B.; Johnstone, J. C.; Pereira, N. *Chem Eng Sci* **2002**, *57*, 2101.
(182) Harvey, A. P.; Mackley, M. R.; Stonestreet, P. *Ind Eng Chem Res* **2001**, *40*, 5371.
(183) Harvey, A. P.; Mackley, M. R.; Seliger, T. *J Chem Technol Biot* **2003**, *78*, 338.
(184) Vilar, G.; Williams, R. A.; Wang, M.; Tweedie, R. J. *Chem Eng J* **2008**, *141*, 58.
(185) Lobry, E.; Lasuye, T.; Gourdon, C.; Xuereb, C. *Chem Eng J* **2015**, *259*, 505.
(186) Smith, K. B.; Mackley, M. R. *Chem Eng Res Des* **2006**, *84*, 1001.
(187) Reis, N.; Harvey, A. P.; Mackley, M. R.; Vicente, A. A.; Teixeira, J. A. *Chem Eng Res Des* **2005**, *83*, 357.
(188) Reis, N.; Vincente, A. A.; Teixeira, J. A.; Mackley, M. R. *Chem Eng Sci* **2004**, *59*, 4967.
(189) Reis, N.; Vicente, A. A.; Teixeira, J. A. *Chem Eng Process* **2010**, *49*, 793.
(190) Zheng, M. Z.; Mackley, M. *Chem Eng Sci* **2008**, *63*, 1788.
(191) Lopes, A. M.; Silva, D. P.; Vicente, A. A.; Pessoa, A.; Teixeira, J. A. *J Chem Technol Biot* **2011**, *86*, 1159.
(192) Reis, N.; Goncalves, C. N.; Aguedo, M.; Gomes, N.; Teixeira, J. A.; Vicente, A. A. *Biotechnol Lett* **2006**, *28*, 485.
(193) Reis, N.; Goncalves, C. N.; Vicente, A. A.; Teixeira, J. A. *Biotechnol Bioeng* **2006**, *95*, 744.
(194) Reis, N.; Mena, P. C.; Vicente, A. A.; Teixeira, J. A.; Rocha, F. A. *Chem Eng Sci* **2007**, *62*, 7454.
(195) Reis, N.; Pereira, R. N.; Vicente, A. A.; Teixeira, J. A. *Ind Eng Chem Res* **2008**, *47*, 7190.
(196) Phan, A. N.; Harvey, A. P.; Rawcliffe, M. *Fuel Process Technol* **2011**, *92*, 1560.
(197) Zheng, M.; Skelton, R. L.; Mackley, M. R. *Process Saf Environ* **2007**, *85*, 365.
(198) Mohd Rasdi, F. R. P., A. N.; Harvey, A. P. *Chem Eng J* **2013**, *222*, 282.
(199) Castro, F.; Ferreira, A.; Rocha, F.; Vicente, A.; Teixeira, J. A. *Aiche J* **2013**, *59*, 4483.
(200) Castro, F.; Ferreira, A.; Rocha, F.; Vicente, A.; Teixeira, J. A. *Ind Eng Chem Res* **2013**, *52*, 9816.
(201) Phan, A. N.; Harvey, A. *Chem Eng J* **2010**, *159*, 212.
(202) Phan, A. N.; Harvey, A.; Lavender, J. *Chem Eng Process* **2011**, *50*, 254.
(203) Phan, A. N.; Harvey, A. P.; Eze, V. *Chem Eng Technol* **2012**, *35*, 1214.
(204) Phan, A. N.; Harvey, A. P. *Chem Eng J* **2011**, *169*, 339.
(205) Phan, A. N.; Harvey, A. P. *Chem Eng J* **2012**, *180*, 229.
(206) Solano, J. P.; Herrero, R.; Espin, S.; Phan, A. N.; Harvey, A. P. *Chem Eng Res Des* **2012**, *90*, 732.
(207) Chew, C. M.; Ristic, R. I.; Dennehy, R. D.; De Yoreo, J. J. *Cryst Growth Des* **2004**, *4*, 1045.
(208) Ristic, R. I. *Chem Eng Res Des* **2007**, *85*, 937.
(209) Ni, X. W.; Liao, A. T. *Cryst Growth Des* **2008**, *8*, 2875.
(210) Ni, X. W.; Liao, A. T. *Chem Eng J* **2010**, *156*, 226.
(211) Ni, X. W.; Valentine, A.; Liao, A. T.; Sermage, S. B. C.; Thomson, G. B.; Roberts, K. J. *Cryst Growth Des* **2004**, *4*, 1129.
(212) Callahan, C. J.; Ni, X. W. *Crystengcomm* **2014**, *16*, 690.
(213) Callahan, C. J. N., X. W. *Can J Chem Eng* **2014**, *92*, 1920.
(214) Brown, C. J.; Ni, X. W. *Cryst Growth Des* **2011**, *11*, 3994.
(215) Brown, C. J.; Ni, X. W. *Cryst Growth Des* **2011**, *11*, 719.

(216) Brown, C. J.; Ni, X. W. *Crystengcomm* **2012**, *14*, 2944.
(217) Nývlt, J. *J Cryst Growth* **1968**, *3-4*, 377.
(218) Kobari, M.; Kubota, N.; Hirasawa, I. *Crystengcomm* **2013**, *15*, 1199.
(219) Brown, C. J. L., Y. C.; Nagy, Z. K.; Ni, X. *Crystengcomm* **2014**, *16*, 8008
(220) Zettler, H. U.; Weiss, M.; Zhao, Q.; Müller-Steinhagen, H. *Heat Transfer Eng* **2005**, *26*, 3.
(221) Middis, J.; Paul, S. T.; Müller-Steinhagen, H. M. *Heat Transfer Eng* **1998**, *19*, 36.
(222) Majumder, A.; Nagy, Z. K. *Cryst Growth Des* **2015**, *15*, 1129.
(223) Briggs, N. E. B. Schacht, U.; Raval, V.; McGlone, T.; Sefcik, J.; Florence, A. J. *Org Process Res Dev* **2015**, *Submitted.*
(224) Siddique, H. H., I.; Florence, A. J. *Org Process Res Dev* **2015**, *Submitted.*
(225) Jawor-Baczynska, A. M., P.; Sefcik, J. *Org Process Res Dev* **2015**, *Submitted.*